AD-A055 641 AIR FORCE INST OF TECH WRIGHT-PATTERSON AFB OHIO SCH--ETC F/G 17/5
ANALYSIS AND COMPARISON OF MODULATION SCHEMES FOR A LASER LINE --ETC(U)
DEC 77 W B TOWNSEND

UNCLASSIFIED AFIT/GEO/EE/77-7 NL

1 OF 1
AD
A055 641

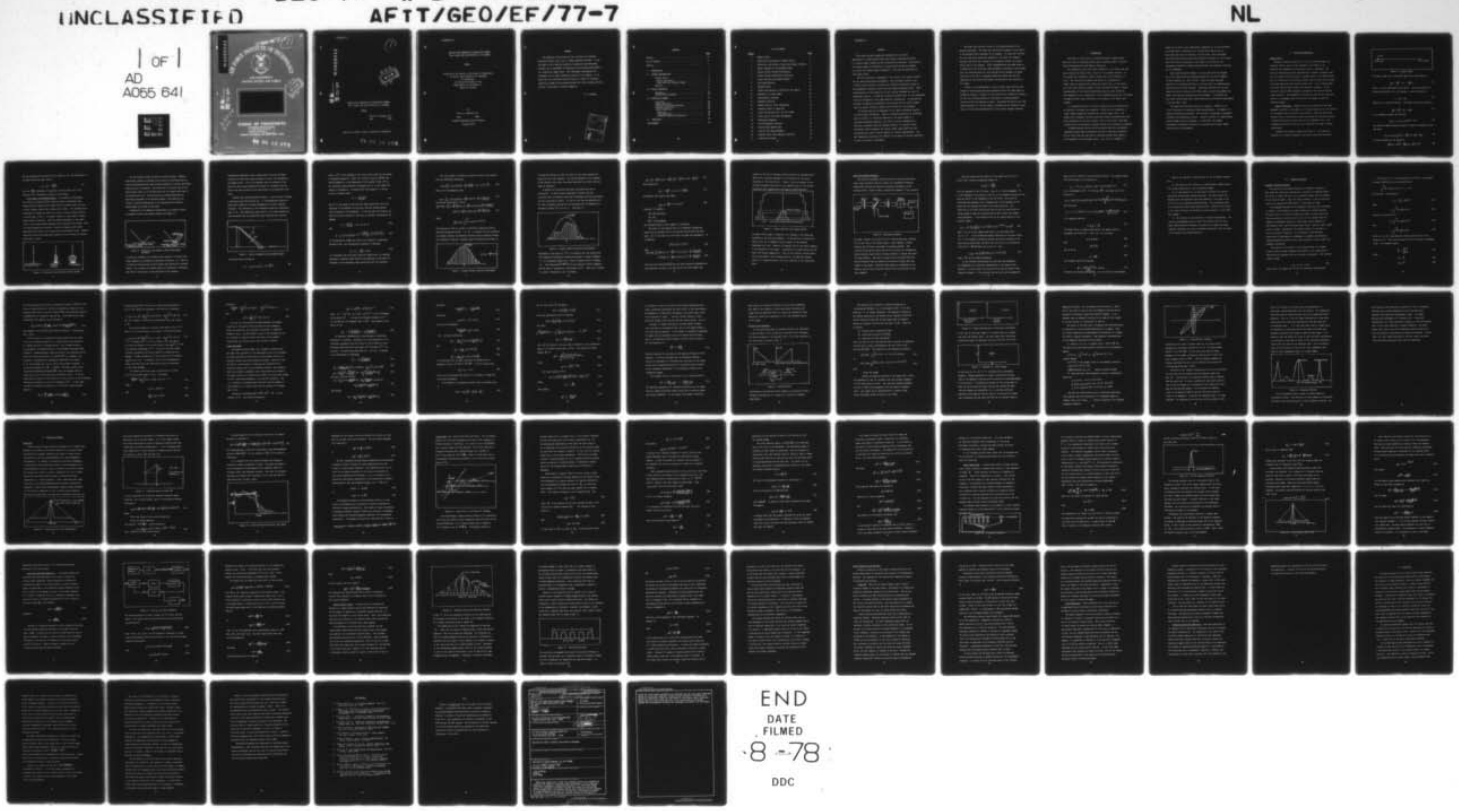

END
DATE FILMED
8-78
DDC

AIR FORCE INSTITUTE OF TECHNOLOGY

AIR UNIVERSITY
UNITED STATES AIR FORCE

See back page for 1473

SCHOOL OF ENGINEERING

WRIGHT-PATTERSON AIR FORCE BASE, OHIO

GEO/EE/77-7

ANALYSIS AND COMPARISION OF MODULATION SCHEMES FOR A LASER LINE SCAN SYSTEM AT 10.6 MICRONS

THESIS

Willie B. Townsend, B.S.
Capt USAF

Approved for public release; distribution unlimited.

GEO/EE/77-7

ANALYSIS AND COMPARISON OF MODULATION SCHEMES FOR A LASER LINE SCAN SYSTEM AT 10.6 MICRONS

THESIS

Presented to the Faculty of the School of Engineering
of the Air Force Institute of Technology
Air University
in Partial Fulfillment of the
Requirements for the Degree of
Master of Science

by

Willie B. Townsend, B.S.
Capt USAF
Graduate Engineering Electro-Optics

December 1977

PREFACE

The emphasis of this study was the selection of a suitable modulation scheme from a list of common modulation schemes. It was not meant to be a detailed analysis of modulation and processing systems, but an assessment of modulation and processing requirements for prospective signal types. This assessment supplemented the assessment of the range estimation accuracy of the signals. It is hoped that the information provided herein is useful in selecting modulation schemes and processing systems that afford ranging accuracy without a high degree of system complexity.

W. B. Townsend

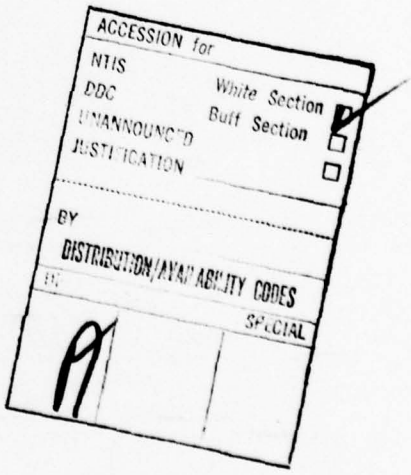

CONTENTS

LIST OF FIGURES

ABSTRACT

This paper provides background information to aid in the application of carbon dioxide lasers and optical heterodyne receivers to a proven target recognition and reconstruction technique. Specifically this paper weighs the feasibility of using various modulation schemes to provide the required range information. This goal was approached in three major steps.

The first step was an assessment of the nature of the signal receiver and the system operational environment. The heterodyne receiver, with a strong local oscillator, recovers the transmitted modulation signal at an intermediate frequency carrier and with additive gaussian noise. These characteristics of the signal out of the receiver determine the type of processing required. In addition a doppler frequency shift of the transmitted field was determined to have some important consequences. It required the allowance of additional bandwidth at the receiver and for certain signal types the doppler adversely impacts the efficiency of the processor.

The second step was an assessment of the signal processing required to provide range information. Range is estimated indirectly by estimating time of arrival of a repetitive waveform or the phase change of a continuous sinusoidal waveform. For time of arrival estimation of a waveform in gaussian noise the optimum processor is a matched filter. The matched filter responses for various signal types (which are well documented) were used to select signals for further consideration. The most important criteria was the ability of the signal to provide resolution in time of arrival or time delay.

The final step involved a study of the characteristics of the selected waveforms. The study was concentrated primarily on the nature of the matched filter responses of the signals. Of particular interest were the time delay resolution capability, the effect of a doppler frequency shift and the flatness of the response outside the central (main) lobe of the response. Final recommendations were made based on a comparison of the predicted range estimation accuracies of each signal type, the characteristics of their matched filter response (or phase lock loop in the case of sinusoidal amplitude modulation) and the complexity of the system requirements for generation and detection of the signal.

Anlysis of the performance of various signal types indicate that signals of equal energy and equal bandwidth provide the same degree of estimation accuracy. Because of this selection of a modulation scheme is in this case influenced mainly by complexity of system operation associated with the modulation scheme. Sinusoidal AM requires the least system complexity of all the signals considered and is therefore a good choice for near-term implementation of the subject ranging technique.

I. Introduction

The object of this study is a proposed airborne ranging system which will scan an extended ground target providing target to aircraft range information with high angular resolution.

The transmitter will scan a path transverse to the flight path and upon reaching the lateral limit, return to the original position. In this manner the transmitter covers a large path of the terrain as it flies. The receiver will measure and record the transmitter to target range at regular points along the lateral scan. If the points are color coded (different shades of gray according to range) a contour representation of the terrain and objects along the path covered by the transmitter can be constructed. This information along with reflectance information gives a good indication of the nature of the target area scanned.

To accomplish the goal of contour reconstruction the receiver will be required to estimate two parameters. These are the transmitter to target signal propagation time and the received signal level. The signal level estimation involves relatively simple processing while time delay estimation can be quite complex. Thus in this report time delay estimation will be discussed in greater detail than reflectance estimation.

Scanning systems such as the one described have been successfully implemented using laser illuminators and direct detection techniques. As yet little work has been done in analyzing systems which employ a 10.6 micrometer (μm) wavelength source. One void, for example, is

caused by the lack of any comprehensive comparison of the effectiveness of various types of modulation for a system operating at 10.6 μm. This study will serve to partially fill the void. Since heterodyne detection would be used, phase and frequency information in the received laser field will be available at the output of the detector and consequently modulation schemes involving phase and frequency variations can be considered.

This study and others similar to it are spurred by the growing use of CO_2 lasers which are finding applications in optical communications, ranging, etc. (Ref. 12:221). There are some very good reasons for the growing popularity of the CO_2 lasers in communications (particularly for mobile systems). Operating conditions for the CO_2 lasers are not as critical as for other lasers, vacuum requirements are simple, and optical tolerances are less stringent. In addition the CO_2 lasers provide high output power operating at efficiencies approaching 15 percent (Ref. 1:18).

The paper has three main sections or chapters. Chapter II is a brief discussion of important system considerations. In Chapter III signal processing is discussed. This includes a discussion of parameter estimation and estimation accuracy. Finally in Chapter IV, Applications, various signal types are examined. In particular, the signal performance in parameter estimation is predicted and peculiar signal characteristics are examined.

II. Systems Consideration

Doppler Effect

Because a coherent receiver is to be used, unwanted phase and frequency effects caused by the atmosphere, the target or the modulator and transmitter instabilities, must be considered. One effect which deserves special consideration is doppler frequency shift due to aircraft velocity relative to ground targets. The doppler shift will be a function of the aircraft velocity and the angle that the beam centerline makes with the aircraft flight path. For a scanning beam this angle and the doppler shift are constantly changing. At the receiver a doppler shift presents a problem for the detector and the range estimator. The bandwidth of the detector and the IF filter must be able to accommodate such a shift and still manage to pass the modulated signal.

General Definition. Doppler effect can be defined as the time dependent variation of the phase of a received signal due to the velocity of the signal source relative to the receiver. When the source and receiver are co-located such as with an aircraft the effective closing or departing velocity is twice that of the transmitter (i.e., the transmitter and the receiver are both closing on the target at equal velocities).

Consider the situation depicted in Figure 1. The round trip distance for a signal traveling to the point target and back is 2L.

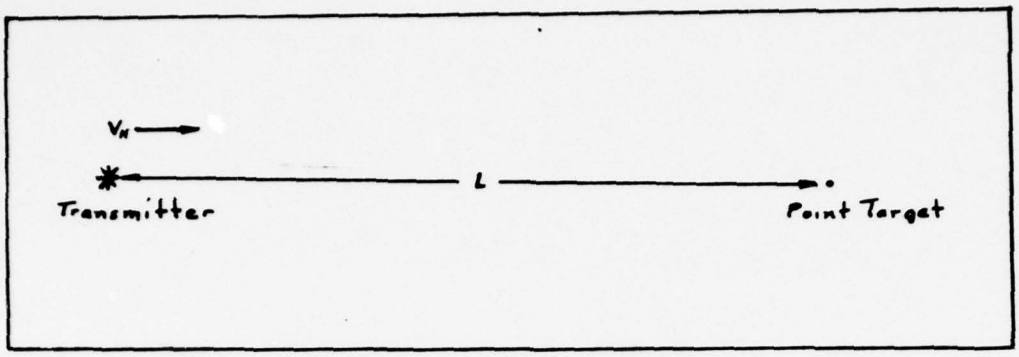

Figure 1. Doppler Effect

The phase change for a continuous signal over this length is

$$\phi = \frac{2\pi}{\lambda} \cdot 2L = \frac{4\pi}{\lambda} L \tag{1}$$

where λ is the wavelength of the signal. Since the aircraft is moving with velocity V_H the distance L can be written as

$$L = D_o - V_H t \tag{2}$$

Where D_o is a constant distance. The phase can now be written as

$$\phi = \frac{4\pi}{\lambda} (D_o - V_H t) \tag{3}$$

If a transmitted signal has the form

$$S'(t) = A' \cos (2\pi f_o t + \theta) \tag{4}$$

the received signal having traveled the round trip distance L has the form

$$S(t) = A \cos \left[2\pi f_o t - \frac{4\pi}{\lambda} (D_o - V_H t) + \theta'\right] \tag{5}$$

so that the phase of the signal is

$$\phi(t) = 2\pi f_o t - \frac{4\pi}{\lambda} (D_o - V_H t) + \theta' \tag{6}$$

and the instantaneous frequency of the signal is the time derivative of the phase divided by 2π, that is

$$f_i = f_o - \frac{2V_M}{\lambda} \tag{7}$$

The term $\frac{2V_M}{\lambda}$ represents the apparent frequency shift due to the velocity of the transmitter relative to the target.

Facet Model and Extended Targets. The problem of determining the effects of target-aircraft velocity becomes considerably more complex when the signal return comes from an extended target or group of point targets rather than a single point target. The problem can be simplified by viewing the target as a series of small planar surfaces or facets (Ref. 1:25-7). For smooth surfaces a large number of small facets would be required. Since the signal wavelength is very small (10.6 μ) even fairly smooth surfaces can be described with facets. With the surface modeled as a series of facets the signal return can be described as the sum of the returns from the individual facets. Figure 2 shows the return from plane waves incident on flat surfaces of various sizes (Ref. 1:25-7).

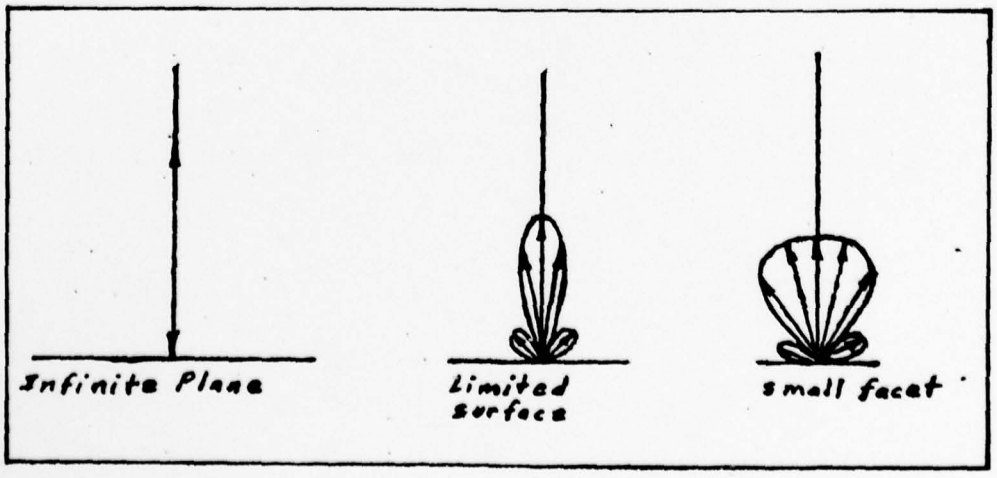

Figure 2. Reflection from Normally Incident Fields

For the infinite plane the return is unidirectional. However, plane waves incident on limited flat surfaces are diffracted and the return is multidirectional with varying strengths for various directions from the point of incidence. The centerline of the main lobe of the return from a facet is in the direction that the signal would take if the surface were flat. Two factors are of primary importance in affecting the spread of the reflected signal. The spread of the return is directly proportional to the wavelength and inversely proportioned to the size of the facet.

Backscatter is an important consideration for signals trained on targets at other than normal incident (see Figure 3).

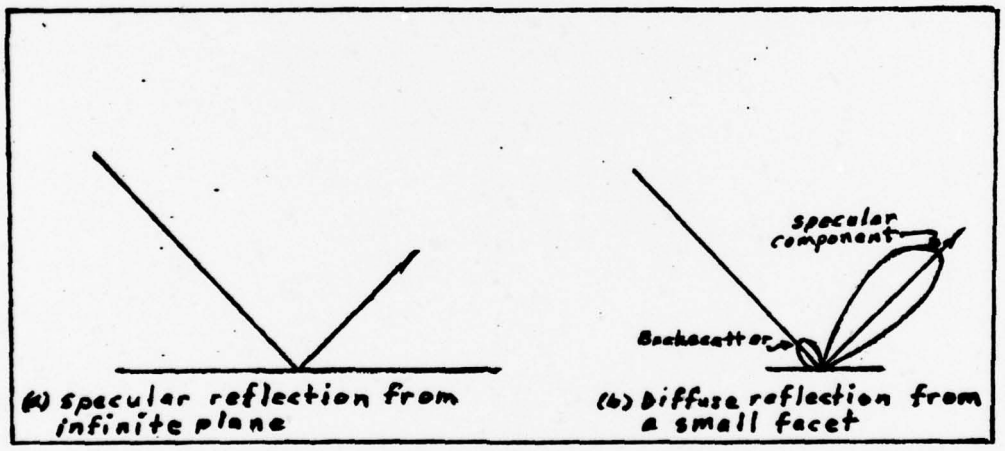

Figure 3. Reflection from Fields at Other Than Normal Incidence

A plane wave incident on an infinite flat surface or a surface very large compared to wavelength is specularly reflected, i.e., there is no return in the direction of the receiver and therefore no received signal. For a surface of limited extent the reflection is diffused and there is some return in the direction of the receiver.

Consequently backscatter from a single small facet with incident radiation at other than normal incidence is due to the spreading of the signal return. Thus it is apparent that the strength of the return to the receiver depends on the angle of incidence, and the size of the facet as well as the reflectance of the material of the facet.

Consider the situation shown in Figure 4. The aircraft is flying a horizontal path with velocity V_H. A one-dimensional stretch of ground with length W is being illuminated by a beam of angular width $\Delta\gamma$. The centerline of the transmitted beam has a depression angle of γ_o. Here depression angle refers to the angle between the beam centerline and the horizontal plane containing the aircraft.

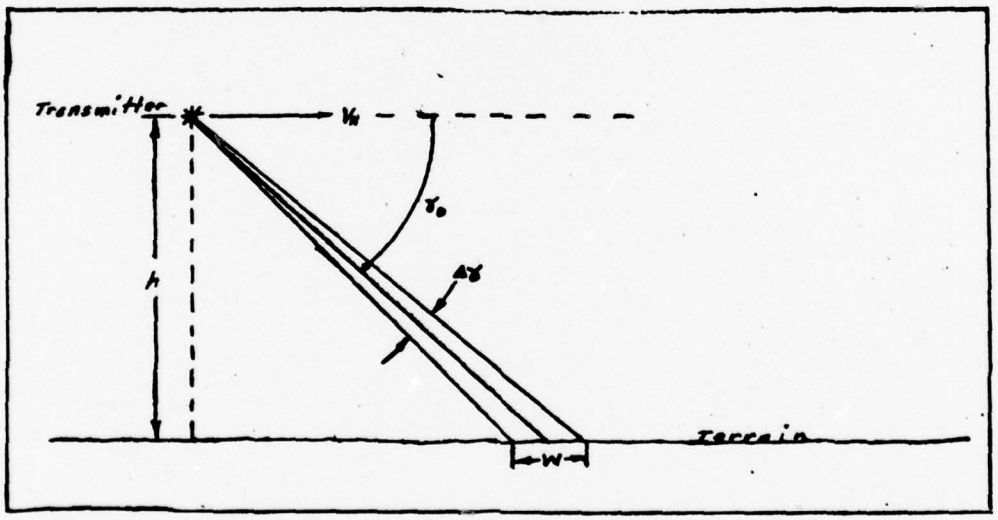

Figure 4. Mobile Transmitter and Extended Target

The return from one facet is

$$E_i = e_i \rho_i \cos\left(\omega t - 2\pi \frac{2r_i}{\lambda}\right) \tag{8}$$

where $e_i \rho_i$ is the strength of the return from a point on the ground at depression angle γ_i, where γ_i is greater than $\gamma_o - \Delta\gamma$ and less than $\gamma_o + \Delta\gamma$ and e_i is the amplitude of the incident field. ρ_i is the reflection (and backscatter strength) and r_i is the range from target to transmitter. In Equation (8) the parameter r_i can be written in another form,

$$r_i = \frac{(h + n_i)}{\sin \gamma_i} \tag{9}$$

Here h is the height of the aircraft above ground and n_i is the deviation of the midpoint of the facet from the average ground level (from which h is measured). If the aircraft has velocity V_H then its velocity relative to the facet is $V_H \cos \gamma_i$ and Equation (8) becomes

$$r_i = \frac{h + n_i}{\sin \gamma_i} - V_H \cos \gamma_i \, t + \tag{10}$$

and

$$E_i = e_i \rho_i \cos\left[2\pi f_o t - 2\pi \frac{2\left(\frac{h + n_i}{\sin \gamma_i} - V_H \cos \gamma_i \, t\right)}{\lambda}\right] \tag{11}$$

If the derivation of ϕ_i (the term in the brackets) is taken and divided by 2π, the instantaneous frequency is obtained,

$$f_i = f_o + \frac{2 V_H}{\lambda} \cos \gamma_i \tag{12}$$

It is apparent that the return from this single facet or scatterer undergoes a frequency shift and that the magnitude of the shift is dependent on the depression angle associated with the scatterer.

The total signal at receiver is simply the sum of the returns from the individual scatterers,

$$s(t) = \sum_i e_i \rho_i \cos\left[2\pi f_o t - \frac{4\pi}{\lambda}\left(\frac{h + n_i}{\sin\gamma_i} - V_H \cos\gamma_i\, t\right)\right] \tag{13}$$

This can be rearranged to give

$$s(t) = \sum e_i \rho_i \cos\left[2\pi\left(f_o + \frac{2V_H}{\lambda}\cos\gamma_i\right)t - \frac{4\pi}{\lambda}\left(\frac{h + n_i}{\sin\gamma_i}\right)\right] \tag{14}$$

The Fourier transform of $s(t)$ is

$$\mathcal{F}_t[s(t)] = \sum e_i \frac{\rho_i}{2}\left\{\delta\left(f - f_o - \frac{2V_H}{\lambda}\cos\gamma_i\right)\exp\left[j\frac{4\pi}{\lambda}\left(\frac{h + n_i}{\sin\gamma_i}\right)\right]\right.$$
$$\left. + \delta\left(f + f_o + \frac{2V_H}{\lambda}\cos\gamma_i\right)\exp\left[-j\frac{4\pi}{\lambda}\left(\frac{h + n_i}{\sin\gamma_i}\right)\right]\right\} \tag{15}$$

where

$$\mathcal{F}_t[s(t)] = \int_{-\infty}^{\infty} s(t)\exp[-j2\pi f t]\, dt$$

The spectrum of $s(t)$ is a series of discrete frequencies with an envelope determined by $e_i \rho_i$. If ρ_i is constant and the scatterers are roughly uniform, the spectrum envelope would be gaussian because the transmitted beam has a gaussian power distribution (see Fig. 5).

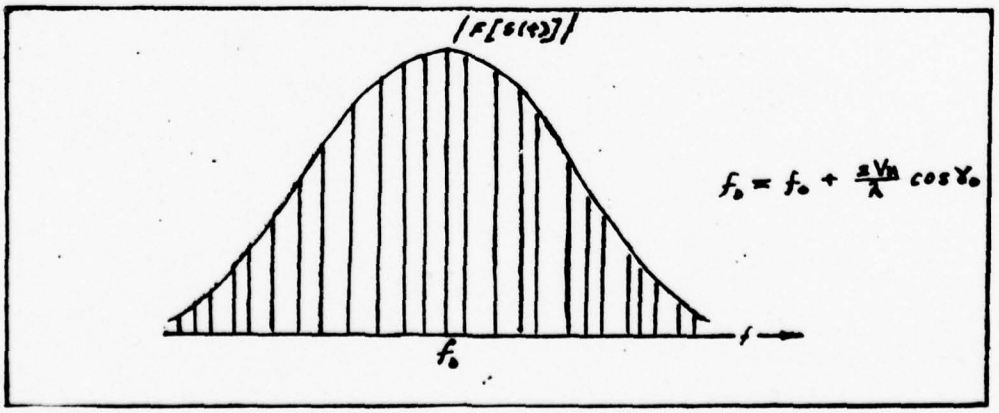

Figure 5. Doppler Spread (uniform reflectance)

It should be pointed out that the lines are not evenly spaced and should be very close together. The spacing depends on the roughness of the surface, since each line shown represents the return from one facet or scatterer.

In general the situation previously described will not be encountered. It would be more reasonable to expect that the scatterers are of different sizes and inclinations and the reflectance may vary from point to point. If that is the case the spectrum will not have a gaussian envelope but the envelope will be bounded by an envelope in which $\rho_i = 1$ for all i . (See Fig. 6.)

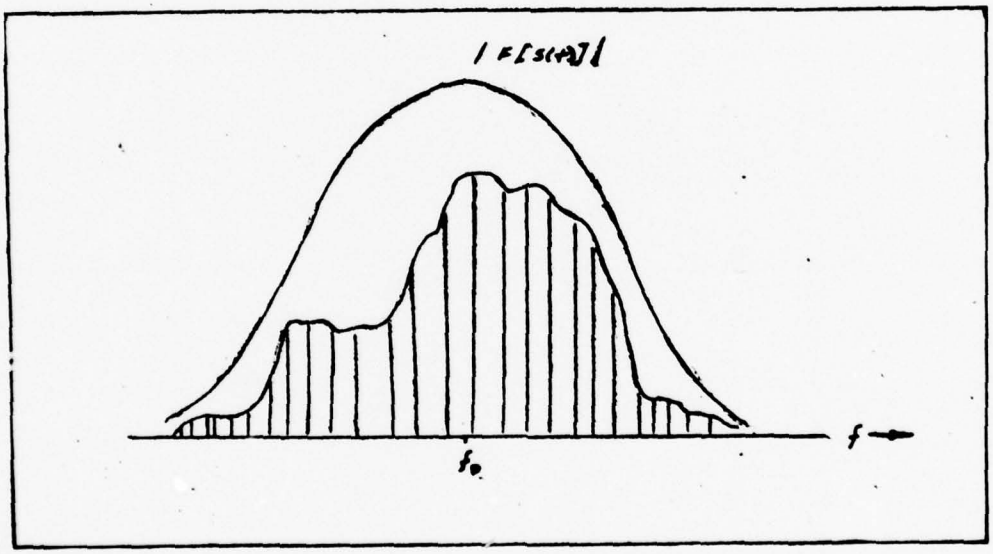

Figure 6. Doppler Spread (nonuniform reflectance)

Regardless of the nature of ρ_i it is apparent that the return from the originally monochromatic unmodulated signal of single frequency f_o is a modulated signal with a center frequency which is roughly f_o . The frequency $f_D = f_o + \frac{2V_R}{\lambda} \cos\gamma_0$ is the apparent carrier frequency and the band of frequencies is determined by $\Delta\gamma$. This can be related to a band of frequencies Δf as follows:

$$\Delta f = \left[f_o + \frac{2V_H}{\lambda}\cos\left(\gamma_o - \frac{\Delta\gamma}{2}\right)\right] - \left[f_o + \frac{2V_H}{\lambda}\cos\left(\gamma_o + \frac{\Delta\gamma}{2}\right)\right] \tag{16}$$

which reduces to

$$\Delta f = \frac{4V_H}{\lambda}\sin\gamma_o \sin\left(\frac{\Delta\gamma}{2}\right) \tag{17}$$

Furthermore since $\Delta\gamma$ is very small

$$\Delta f \cong \frac{2V_H}{\lambda}\sin\gamma_o\,\Delta\gamma \tag{18}$$

Consider, for example,

V_H = 800 meters/sec

γ_o = 85°

$\Delta\gamma$ = 5 milliradians

The frequency band for this example is 751,845 Hz.

The effect of the doppler shift on a modulated transmitted signal can be accounted for by letting the factors $\{e_i\}$ vary with time. All of the terms (e_i) will have the same time dependence. If in addition

$$\mathcal{F}[e_i(t)] = E(f) \tag{19}$$

then

$$\mathcal{F}[S_r(t)] = \sum_i P_i E_i\left(f - f_o - \frac{2V_H}{\lambda}\cos\gamma_i\right)\exp\left[-j\frac{4\pi}{\lambda}\frac{(h+n_i)}{\cos\gamma_i}\right] + P_i E_i\left(f + f_o + \frac{2V_H}{\lambda}\cos\gamma_i\right)\exp\left[-j\frac{4\pi}{\lambda}\frac{(h+n_i)}{\cos\gamma_i}\right] \tag{20}$$

Since all the functions $E_i(f)$ have the same frequency dependence but with different strengths, the spectrum of the total signal will

consist of the sum of identical forms multiplied by varying factors which have a gaussian dependence on the distance of the center frequency of the form from f_o . Figure 7 gives an example of what the spectrum might look like for the unlikely case of five uniform scatterers and a signal with a rectangular shaped spectrum.

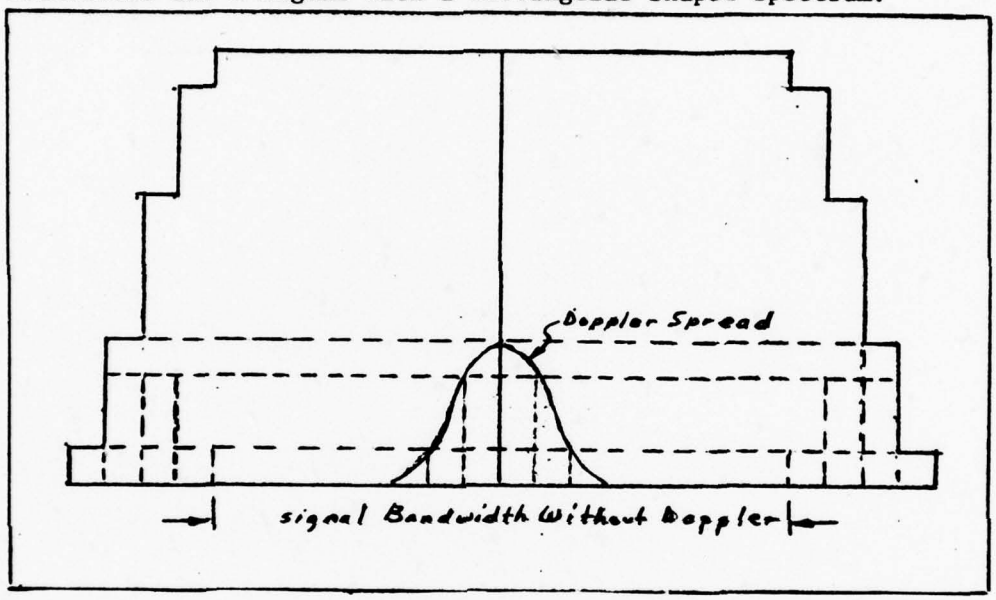

Figure 7. Square Spectrum with Doppler Spread

The major effect might be expected to be rounding of the edges and spreading of the sides and pedestal. In any practical situation the effects will not be symmetric and the phases of the separate components will vary. However, the doppler will be very small compared to the bandwidth of the signal. Consequently the edge effects will be minor even though asymmetrical. Thus for the coherent receiver which will be described in the following section, the important doppler effect is a frequency shift of the total spectrum of the transmitted field.

Optical Heterodyne Receiver

The optical heterodyne receiver mixes the received field with a laser local oscillator field to produce an intermediate frequency signal which retains the phase and frequency information of the received field. Figure 8 shows a simplified schematic of the receiver.

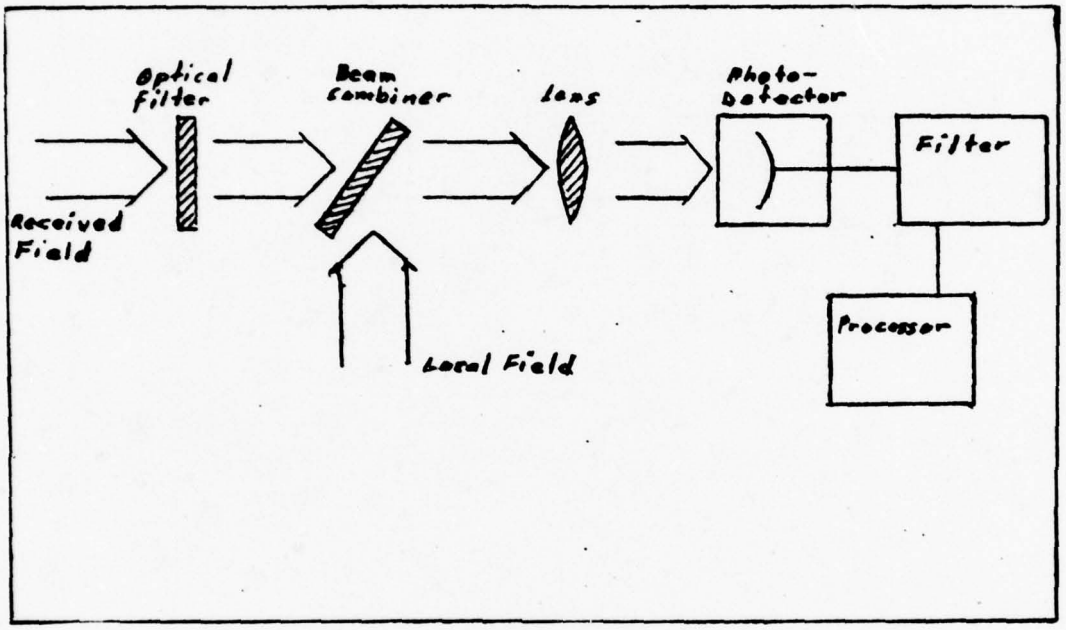

Figure 8. Heterodyne Receiver

The model consists of an optical filter (narrow band pass, centered at 10.6 μm), one or two convex lenses, a beam combiner, a photo detector and IF filter, and signal processing hardware. The received field and the field from the local source are refracted by either separate lenses before the beam combiner or single lens after the beam combiner. The lens or lenses are so positioned that the optical distance from the lenses to the detector equals the focal length of the lenses. Received field energy is transmitted to the detector and the local field is reflected onto the detector by the beam combiner.

The noise power spectral density of the signal out of the IF filter (for a properly normalized signal) is

$$N(f) = \frac{h f_o}{4 \eta} \tag{21}$$

over the passband of the IF filter. Here h is Plancks constant f_o is the frequency of the optical field, η is the quantum efficiency of the detector and W is the bandwidth of the IF filter. This noise is stationary and gaussian, and it depends only on the frequency of the signal and the quantum efficiency of the photo detector. The condition for the noise having this form is that the local field be strong enough to make the contributions of dark current and thermal noise negligible. A very general form for the signal portion of the receiver output

$$i(t) = Re\left\{\frac{1}{A_d}\iint_{A_d} U_r(x,y,t)\, U_{Lo}^{*}(x,y)\, e^{-j2\pi f_{io} t}\, dx\, dy\right\} \tag{22}$$

where $U_r(x,y)$ is the complex amplitude of the received field, $U_{Lo}(x,y)$ is the normalized complex amplitude of the local field, f_{io} is the frequency difference between the optical carriers of the local and received field, and A_d is the active area of the detector. If $U_r(x,y,t) = \sqrt{P_r}\, U(t)$ and $U_{Lo}(x,y) = 1$ then

$$i(t) = Re\left\{\sqrt{P_r}\, U(t) \exp[-j2\pi f_{io} t]\right\} \tag{23}$$

where $U(t)$ is the signal modulation.

In all previous calculations the field has been assumed to be propagating in a direction perpendicular to the plane of the detector. In other words, the received field and the detector were spatially aligned. If the detector and the field are misaligned the

signal onto the detector can be seriously reduced. For example assume the field incident on the detector is

$$U_r = A(x,y) \exp[jk \sin\phi x + jk \cos\phi z]\, U(t) \tag{24}$$

for a misalignment of ϕ. For $A(x,y) = \sqrt{P_r}$, the signal out of the detector is

$$y_s(t) = Re\{U(t) \exp[-jk\cos\phi z - j2\pi f_{if} t]\sqrt{P_r} \iint_{D/2}^{D/2} \exp[jk \sin\phi x]\, dx\, dy \tag{25}$$

and this gives

$$y_s(t) = Re\{D^2 U(t) \exp[-j2\pi f_{if} t]\sqrt{P_r}\} \frac{\sin(\frac{k}{2} D \sin\phi)}{\frac{k}{2} D \sin\phi} \tag{26}$$

It is apparent that for

$$\sin\phi = \lambda/D \tag{27}$$

the signal level is reduced drastically; the signal level is negligible for $\sin\phi \geq \lambda/D$. Since λ/D is very small

$$\sin\phi \cong \phi \tag{28}$$

and

$$\phi \leq \lambda/D \tag{29}$$

Now if we let

$$D = \sqrt{A_d} \tag{30}$$

and consider that $\lambda = 10.6$ microns

$$\phi < \frac{10.6 \times 10^{-6}\, m}{\sqrt{A_d}} \text{ radians} \tag{31}$$

Therefore the maximum misalignment is on the order of milliradians.

Some of the important characteristics of the heterodyne receiver are:

a) The output of the receiver is a nonstationary random process with a mean proportional to the information signal.

b) In the presence of a strong local oscillator the receiver approaches quantum noise limited operation. The dark current and thermal noise are negligible and noise apparent to the input of the IF filter is zero mean-white-gaussian noise. The measurement noise can be modeled as band-limited gaussian noise. Because of the effect of the local oscillator the receiver is very sensitive; it can detect weak signals.

c) The receiver is very sensitive to spatial misalignment. The limits on misalignment serve to limit the receiver field of view. These characteristics determine the nature of the signal processor required, especially the type of estimator which best fills the needs of the system (the optimum detector).

III. Signal Processing

Parameter Estimation Theory

The function of the signal processor is parameter estimation. Both range and reflectance estimates are achieved by estimating signal time delay or round trip time for a transmitted signal and the strength of the received signal. Once time delay is known, it can be related to range by the equation, $R = \frac{c}{2}\tau$ where c is the speed of light.

The a priori knowledge of the parameters time delay and reflectance is limited. The parameters can thus be modeled as random variables. Certainly there is no definite scheme that range and reflectance must follow from point to point and very little can be assumed about the respective probability densities. Reflectance can be expected to vary between 0 and 1 and not beyond these limits. Specific limits cannot be put on range. Depending on the surface, limits of a few feet to tens of feet may be expected. In the absence of more detailed restrictions a high degree of randomness is assumed, and therefore a uniform probability density with a large variance is used to model the parameter statistics.

The output of the receiver, as was shown earlier is a random process with an average component proportional to the signal and an additive noise component which is zero mean and gaussian. The received signal is thus

$$r(t) = s(t) + n(t) \tag{32}$$

where $s(t)$ is the signal and $n(t)$ is the stationary noise process.

The function $r(t)$ can be expressed as the sum of orthonormal functions $\{z_i(t)\}$ which are characterized by

$$\int_{-\infty}^{\infty} z_i(t)\, z_j(t)\, dt = 0 \quad ; \quad i \neq j$$

The function $r(t)$ is given by

$$r(t) = \sum_i r_i\, z_i(t) \tag{33}$$

where

$$r_i = \int_0^{T_p} r(t)\, z_i(t)\, dt \tag{34}$$

Similarly for $n(t)$ and $s(t)$

$$n_i = \int_0^{T_p} n(t)\, z_i(t)\, dt \tag{35}$$

and

$$s_i = \int_0^{T_p} s(t)\, z_i(t)\, dt \tag{36}$$

Where n_i is a zero mean gaussian random variable and T_p is the period of $s(t)$. The received signal $r(t)$ can be written as dependent on $\bar{A}$, the parameter vector

$$\bar{A} = \begin{vmatrix} A_1 \\ A_2 \end{vmatrix} \tag{37}$$

where

$$A_1 = \tau \tag{38}$$

$$A_2 = \rho \tag{39}$$

The received signal would then be written as $r(t,\bar{A}) = s(t,\bar{A}) + n(t)$ Using the representation in (33-36) the probability density for the received signal can be written as $p_{r/A}(r/\bar{A})$ or the probability density of $\{r_i\}$ given the parameters A_1 and A_2. Since $n(t)$ is zero mean and gaussian this density can be written as

$$p_{r/\bar{A}}(r/\bar{A}) = \prod_{i=1}^{k} \frac{1}{\sqrt{\pi N_0}} \exp\left(-\frac{1}{2}\frac{[r_i - s_i(\bar{A})]^2}{N_0/2}\right) \qquad (40)$$

where $N_0/2$ is the two-sided power spectral density in watts/Hz. (Ref. 3:274).

Briefly stated the estimation problem presented by the system is one of estimating parameters of a random nature whose densities are unknown and will be assumed uniform. The optimum processor for parameters of unknown densities is the maximum likelihood (ML) estimator. The ML estimator finds the value of the parameters $\bar{A}$ for which the conditional density of r, $p_{r/\bar{A}}(r/\bar{A})$ is a maximum. The estimator is implemented by maximizing $p_{r/\bar{A}}(r/\bar{A})$ with respect to $\bar{A}$ and choosing that value of $\bar{A}$ as the parameter estimate. It is usually designated as $\hat{A}_i$ (or $\hat{\rho}, \hat{\tau}$). The same results can be obtained by maximizing $\ln p_{r/\bar{A}}(r/\bar{A})$, since the maximum value for either will occur at the same value of $\bar{A}$ (Ref. 3:274). It can be shown that the results of the estimation are not altered if the likelihood function is divided by a factor not dependent on $\bar{A}$. In that light consider the probability function for $r(t)$ with no signal present which is

$$p_{r_n} = \prod_{i=1}^{k} \frac{1}{\sqrt{\pi N_0}} \exp\left[-\frac{1}{2}\frac{r_i^2}{N_0/2}\right] \qquad (41)$$

Dividing $p_{r|\bar{A}}(r/\bar{A})$ by this factor, substituting Equations (2) and (3) and taking the logarithm a new function is obtained,

$$\ln \Lambda_1[r(t), \bar{A}] = \frac{2}{N_0}\int_0^T r(t)\, s(t, \bar{A})\, dt - \frac{1}{N_0}\int_0^T s^2(t, \bar{A})\, dt \qquad (42)$$

The ML estimate can be found by maximizing $\ln \Lambda$, with respect to $\bar{A}$.

The received signal as a function time delay is $s(t-\tau)$ where τ is the time delay of the signal. From this we obtain

$$\ln \Lambda_1[r(t), \tau] = \frac{2}{N_0}\int_0^T r(t)\, s(t-\tau)\, dt - \frac{1}{N_0}\int_0^T s^2(t-\tau)\, dt \qquad (43)$$

If it is assumed that T is large enough so that the signal is within the bounds of the second integral then $\frac{1}{N_0}\int_0^T s^2(t-\tau)\, dt$ is a constant independent of τ. In view of this the second integral in Equation (43) can be ignored in looking for the maximum. The ML estimate for τ is the value of τ for which $\frac{2}{N_0}\int_0^T r(t)\, s(t-\tau)\, dt$ is maximum. This can be implemented by using a matched filter and observing the time of occurrence of the output maximum.

To estimate reflectance take the derivative of $\ln \Lambda_1$ and set the results equal to zero. This gives

$$\frac{\partial \ln \Lambda_1}{\partial \rho} = \frac{2}{N_0}\int_0^T [r(t) + s(t)]\, s'(t)\, dt = 0 \qquad (44)$$

where

$$s'(t) = \frac{1}{\rho}\, s(t) \qquad (45)$$

and

$$\frac{\partial}{\partial \rho}\, s(t) = s'(t) \qquad (46)$$

therefore:

$$\frac{\partial \ln \Lambda_1}{\partial \rho} = \frac{2}{N_o}\int_0^T [r(t)s'(t)]\,dt - \rho\int_0^T [s'(t)]^2\,dt = 0 \tag{47}$$

and

$$\hat{\rho} = \frac{E_r'^2}{N_o}\int r(t)\,s'(t)\,dt \tag{48}$$

For both the reflectance and range estimates the primary concern is to accurately track the point to point change in range and reflection, not necessarily the exact (or absolute) parameter value. In other words if each of the estimates is off by a constant or additive factor the value of the estimate (considering the ultimate use) is not seriously reduced.

Cramer Rao Bound

The Cramer Rao Bound (CRB) for a parameter estimate gives the lower limit possible for the mean-square error of an estimate. The bound provides the lower limit on the estimate error for a parameter using a particular modulation scheme. Because of this the CRB is a useful means of comparing the suitability of a particular signal type for an estimation problem. Any processor which can estimate a parameter with a mean-square-error equal to the CRB is said to be efficient and if there is an efficient estimator for a particular parameter, it is the ML estimator. The ML estimator is asymptotically efficient with the number of observations or in a lesser sense with the energy of the signal (Ref. 3:71).

We begin by designating $\sigma_{A_i}^2 = E[(\hat{A}_i - A_i)^2]$. $\hat{A}_i$ is the estimate of A_i . The Cramer Rao Bound is

$$\sigma_{A_i}^2 = E\left[(\hat{A}_i - A_i)^2\right] \geq J^{ii} \tag{49}$$

where A_1 is ρ and A_2 is τ, and J^{ij} is the ij^{th} element in the matrix J^{-1}. In short the diagonal elements of J^{-1} are the CRB for the estimates (Ref. 3:372). The elements of the matrix J are

$$J_{ij} = E\left[\frac{\partial^2 \ln \Lambda_1}{\partial A_i \partial A_j}\right] = E\left[\frac{\partial^2 \ln \Lambda_1}{\partial \rho \partial \tau}\right] \tag{50}$$

An important consideration in the estimation of multiple parameters is coupling. Coupling is the interdependence of the individual parameters and the effects in the estimates of each. Coupling exists when the cross terms of J and hence J^{-1} are non zero. In other words, when $J_{ij} \neq 0$ for $i \neq j$. Coupling can be determined by evaluating

$$J_{ij} = E\left[\frac{\partial^2 \ln \Lambda_1}{\partial \rho \partial \tau}\right] \tag{51}$$

$$J_{ij} = E\left[\frac{\partial^2}{\partial \rho \partial \tau}\left(\frac{2}{N_0}\int_0^T r(t)\, s(t,\bar{A})\, dt - \frac{1}{N_0}\int_0^T s^2(t,\bar{A})\, dt\right)\right] \tag{52}$$

$$J_{ij} = E\left[\frac{2}{N_0}\int_0^T r(t)\, \frac{\partial^2 s(t,\bar{A})}{\partial \rho \partial \tau}\, dt - \frac{1}{N_0}\int_0^T \frac{\partial^2 s^2(t,\bar{A})}{\partial \rho \partial \tau}\, dt\right] \tag{53}$$

and since $E[r(t)] = s(t,\bar{A})$

$$J_{ij} = \frac{2}{N_0}\int_0^T s(t,\bar{A})\, \frac{\partial^2 s(t,\bar{A})}{\partial \rho \partial \tau}\, dt - \frac{2}{N_0}\int_0^T \frac{\partial^2 s(t,\bar{A})}{\partial \rho \partial \tau}\, s(t,\bar{A})\, dt + \frac{2}{N_0}\int \frac{\partial s(t,\bar{A})}{\partial \rho} \cdot \frac{\partial s(t,\bar{A})}{\partial \tau}\, dt \tag{54}$$

and finally

$$J_{ij} = \frac{2}{N_0}\int \frac{\partial s(t,\bar{A})}{\partial \tau} \cdot \frac{\partial s(t,\bar{A})}{\partial \rho}\, dt \tag{55}$$

and since

$$\frac{\partial s(t,\bar{A})}{\partial \tau} = -\frac{\partial s(t,\bar{A})}{\partial t} \tag{56}$$

also since

$$s(t,\bar{A}) = \rho s'(t,\bar{A}) \tag{57}$$

this can be established

$$\frac{\partial s(t,\bar{A})}{\partial \rho} = \frac{1}{\rho} s(t,\bar{A}) \tag{58}$$

J_{ij} can now be written as

$$J_{ij} = \frac{-2}{\rho N_o}\int_0^T s(t,\bar{A}) \frac{\partial s(t,\bar{A})}{\partial t}\, dt \tag{59}$$

and

$$J_{ij} = \frac{1}{\rho N_o} s^2(t,\bar{A}) \Big|_0^T \tag{60}$$

$$J_{ij} = \frac{1}{\rho N_o}\left[s^2(0,\bar{A}) - s^2(T,\bar{A})\right] \tag{61}$$

It is expected that for most situations the signal will be symmetric so that $s^2(0,\bar{A}) = s^2(T,\bar{A})$. It can be stated that

$$J_{ij} = 0 \; ; \; i \neq j \tag{62}$$

and it may be concluded that there is no coupling for range and reflectance estimates.

In the absence of coupling the lower limit on estimate error is

$$\sigma_{A_i}^2 = \mathrm{Var}\left[\hat{A}_i - A_i\right] \geq J_{ii}^{-1} \tag{63}$$

and for time delay ($\hat{\tau}$) estimates

$$\sigma_\tau^2 \geq \left\{ E\left[\frac{\partial^2}{\partial \tau^2} \ln \Lambda_1 \right] \right\} \tag{64}$$

with some manipulation this is obtained

$$\sigma_\tau^2 \geq \left[\frac{2}{N_0} \int_0^T \left(\frac{\partial}{\partial \tau} s(t,\tau) \right)^2 dt \right]^{-1} \tag{65}$$

and since

$$\int_0^T \left[\frac{\partial s(t,\tau)}{\partial \tau} \right]^2 dt = \int_0^T \frac{\partial^2}{\partial t^2} \left[s(t,\tau) \right] dt = E_r \beta^2 \tag{66}$$

$$\sigma_\tau^2 \geq \frac{N_0}{2 E_r \beta^2} \tag{67}$$

Here β^2 is defined as the mean square bandwidth of the transmitted signal $s(t)$ without noise (Ref. 1:3-10). An equation for determining β^2 is

$$\beta^2 = \frac{\int_{-\infty}^{\infty} (2\pi f)^2 |S(f)|^2 \, df}{\int_{-\infty}^{\infty} |s(f)|^2 \, df} \tag{68}$$

where

$$S(f) = \mathcal{F}\left[s(t) \right] \tag{69}$$

The lower bound for ρ is

$$\sigma_\rho^2 \geq \left\{ \frac{2}{N_0} \int \left[\frac{\partial s(t,\rho)}{\partial \rho} \right]^2 dt \right\}^{-1} = \left\{ \frac{2}{N_0} E_r' \right\}^{-1} \tag{70}$$

where

$$E_r' = \frac{E_r}{\rho^2} \tag{71}$$

This yields

$$\sigma_\rho^2 \geq \frac{N_0 \rho^2}{2 E_r} \tag{72}$$

It is useful to note at this point those signal parameters which effect estimation performance and their effect on that performance. The parameters of significant consequence are system noise, which in the presence of large does not include effects of dark noise and thermal noise, and the received signal energy. For the estimate of target reflectance, the mean square estimate error was seen to be bounded by the ratio of the signal energy to the noise spectral density. If the energy is considered independent of signal type and dependent only on the target and the transmitter, the important system variable is noise spectral density. For this system it is

$$\frac{N_o}{2} = \frac{h f_o}{4 \eta} \tag{73}$$

The only variable for the noise is the quantum efficiency of the detector. It can be concluded that the important limiting factors for estimation at reflectance are the power of the transmitter and the quantum efficiency of the detector both of which can be considered independent of the modulation scheme of the transmitted signal.

The estimate error for time delay (τ) is characterized by

$$\sigma_\tau^2 \geq \frac{N_o}{2 E_r \beta^2} = \frac{h f_o}{4 \eta E_r \beta^2} \tag{74}$$

The important parameters for limiting estimation error are again detector quantum efficiency signal energy and in addition signal mean square bandwidth. If the signals are assumed to have the

same energy, the important parameter is mean square bandwidth. This implies that signals of equal mean square bandwidths and energy have the same time delay (or round trip propagation time) resolution capabilities regardless of the time dependent nature of the signal.

Matched Filter Response

As was shown previously the optimum processor for time delay or range estimate is the correlation or matched filter estimator. The impulse response of the matched filter is the time inversion of the input signal as shown in Fig. 9.

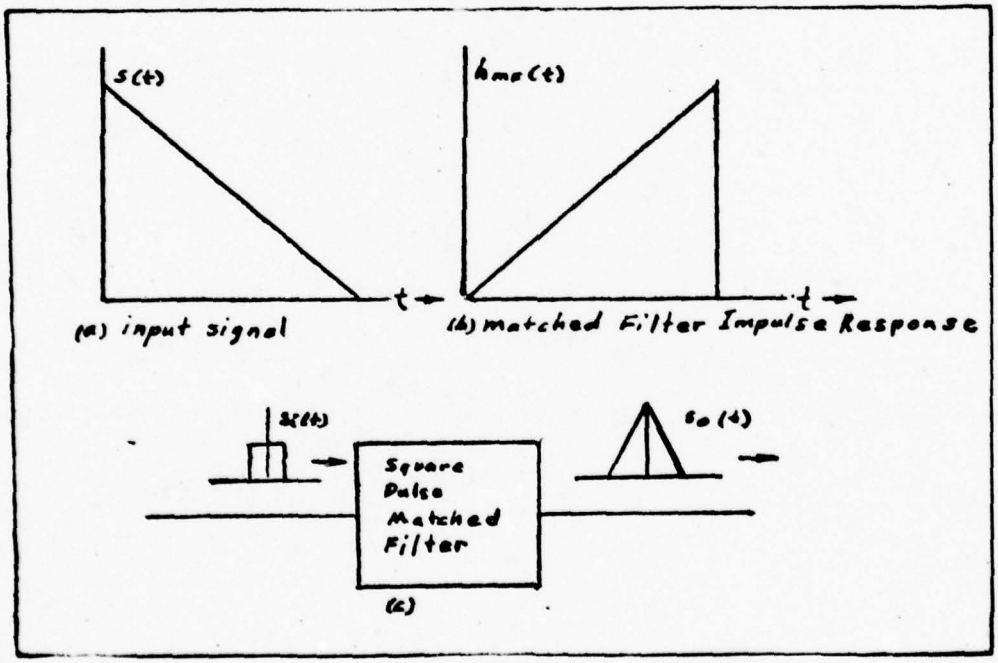

Figure 9. Matched Filter

Calculation of the matched filter response is one means of determining the suitability of a signal for a particular ranging application.

The matched filter response is usually designated as $\chi(\tau, f_d)\exp[j2\pi f_0 \tau]$ where f_d is the doppler shift, τ is time delay and f_0 is carrier frequency. The ambiguity function is the complex amplitude of the matched filter response or $\chi(\tau, f_d)$ Several different forms with various names under the general heading of ambiguity function are used (Ref. 5:119). These are in general

(a) Matched filter response $\chi(\tau, f_d)$

(b) Uncertainty function $|\chi(\tau, f_d)|$

(c) Ambiguity function $|\chi(\tau, f_d)|^2$

From this point on the terms matched filter response and ambiguity function will be used interchangeably and will refer to the function $|\chi(\tau, f_d)|$. The equation for the ambiguity function is

$$|\chi(\tau, f_d)| = \int_{-\infty}^{\infty} s(t)\, s^*(t-\tau)\exp[j2\pi f_d t]\, dt \tag{75}$$

or

$$|\chi(\tau, f_d)| = \int_{-\infty}^{\infty} M^*(f)\, M(f - f_d)\exp[j2\pi f_d \tau]\, dt \tag{76}$$

here

$s(t)$ is the signal

$M(f)$ is the Fourier transform of the signal (Ref. 5:119).

The parameters τ and f_d represent time and frequency mismatch for the signal and the filter. The time and frequency mismatch are due to round trip propagation time and doppler frequency shift. Any target can be characterized by a range of time delays and dopper shifts as shown in Fig. 10(a).

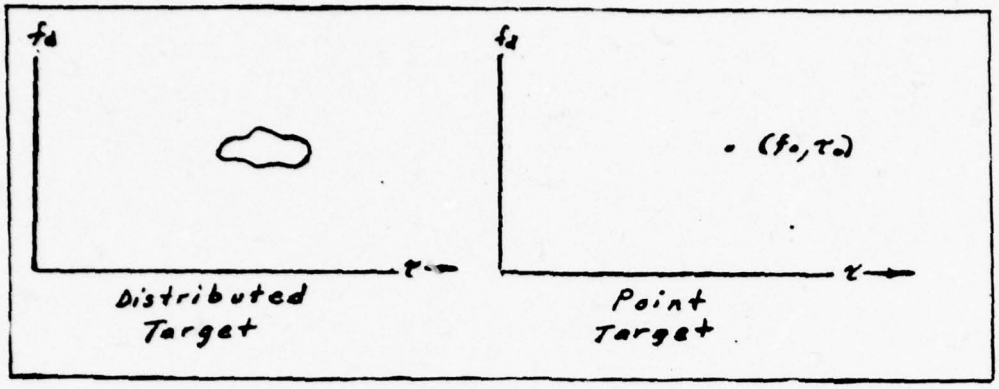

Figure 10. Target Distributions in Time Delay and Doppler

In the case of the point target it is characterized by a single time delay and doppler shift. For this target and a particular transmitted signal the ambiguity function is $|\chi(f_d - f_o, \tau - \tau_o)|$

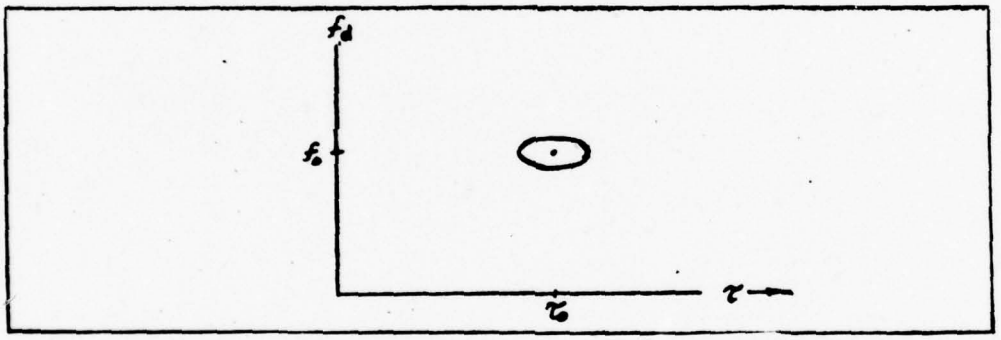

Figure 11. Response of a Point Target

In this case $f_d - f_o$ and $\tau - \tau_o$ represent delay and doppler mismatch. Roughly speaking any targets lying within the main lobe of the ambiguity function will be practically indistinguishable by the receiver. If instead two targets lie far enough apart so that one can be within the main lobe and one outside the main lobe the signals are resolvable, i.e., a receiver perfectly matched to one would not see the other or it would be very small and a searching receiver would see both but as separate lobes or

ambiguity functions. For the purpose of this study f_o and τ_o will be set equal to zero so that the ambiguity function can be observed for arbitrary targets and specific signals. It is apparent that the ambiguity function is the same for all targets. It is just shifted to a particular f_o and τ_o.

The extent of the main lobe in frequency and time delay gives an indication of the resolving capabilities of a signal. This is of major importance in determining the suitability of a signal for delay or doppler estimation. Some important characteristics of the ambiguity function are listed below:

1) When $f_d = 0$, i.e., no doppler shift, $|\chi(f_d, \tau)|$ has the form of the time autocorrelation function of the transmitted signal.

2) $\chi(0,0) = \int_{-\infty}^{\infty} |s(t)|^2 \, dt = \int_{-\infty}^{\infty} |M(f)|^2 \, df = E_s$ (signal energy)

3) $\chi(0,0)$ is the highest point of the ambiguity function.

4) $\chi(\tau, f_d) = \chi(-\tau, -f_d)$

5) $\iint |\chi(\tau, f_d)|^2 \, d\tau \, df_d = E_s$ (implies constant volume)

6) Some important signal-ambiguity function transformation pairs are,

a) $\alpha \, s(\alpha t) \longrightarrow \chi(\alpha\tau, f_d/\alpha)$

b) $M(f) \exp[j\pi p f^2] \longrightarrow \chi(\tau - p f_d, f_d)$

c) $s(t) \exp[j\pi k t^2] \longrightarrow \chi(\tau, f_d + k\tau)$

The last two characteristics are of particular importance. They indicate that the introduction of a quadratic phase (or higher) term, as in linear , causes a shearing of the original ambiguity function.

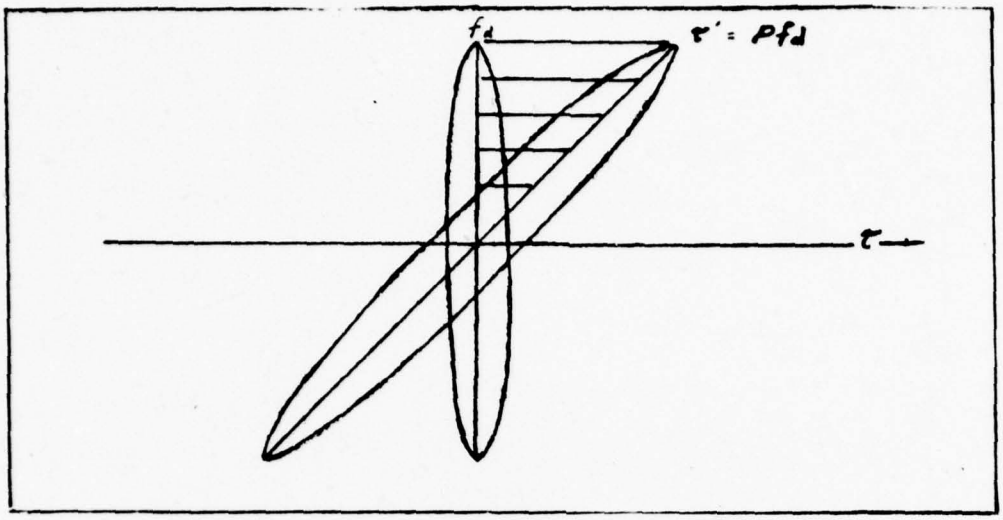

Figure 12. Delay-Doppler Coupling

Consequently for linear or higher order FM any doppler shift displaces the time delay position of the MF response maximum from $\tau = 0$ to $\tau = \rho f_d$. If this does occur then the delay estimate for the signal is biased or specifically it has a constant estimate error of ρf_d. When the doppler mismatch is constant and known the bias can be predicted and accounted for in estimating delay (Ref. 5:123).

Two parts of the mbiguity diagram which will be here defined for use later are the sidelobe and the ambiguity peaks (see Fig. 13). The sidelobe is a subsidiary maxima which is smaller than the main lobe. It poses a problem for some signal types in that it can be mistaken for a nonexistent weak signal and it can mask an existing weak signal. In the presence of additive noise it can appear as high as the main lobe and as such is closer to an ambiguity. In essence the ambiguity peak is a large sidelobe. Its importance is in the fact that its height is very

close to the height of the main lobe and consequently is practically indistinguishable from the mainlobe. The ambiguities limit the range of target distances that can be measured without ambiguity. That is to say the target distribution in time delay cannot exceed the time delay separation of the main lobe and the ambiguity peak. If it does then those parts of atrget which are separated in time delay exactly the same as the main lobe ambiguity separation will appear to have the same range. It is important that the signal be chosen so that the target distribution in time delay is less than or equal to the time delay difference between the main lobe and the ambiguity peak. This distribution limit will be referred to later as the total unambiguous time delay or total unambiguous range for a given signal.

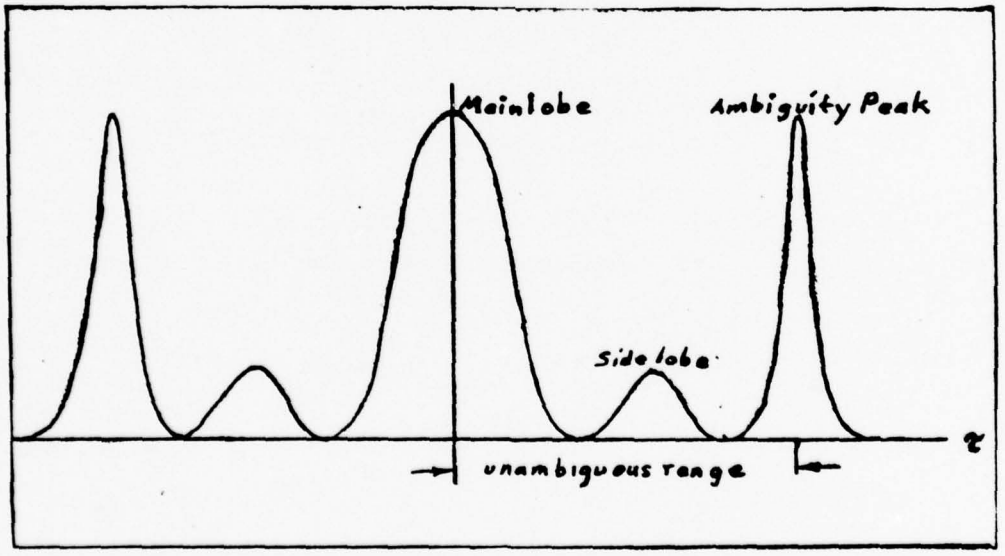

Figure 13. Ambiguity Function

In the following section a number of signal types are discussed in detail. The selection of those signals for discussion was based on the characteristics of their ambiguity function. For

this system the most important requirement is that the ambiguity functions have a narrow high main lobe and good main lobe ambiguity peak separation (unambiguous range). Any signal meeting this requirement is of potential use. A desirable characteristic is a main lobe wide in doppler so that the response level is not overly sensitive to doppler mismatch. The ideal signal would then be one with an ambiguous function which has a main lobe narrow in time delay and constant with doppler. Linear FM, the first signal discussed in the next chapter has characteristics which approaches those noted as desirable.

IV. Modulation Schemes

Linear FM

Simply stated the range resolution capability of a single pulse depends on the width of the pulses formed at the processor output. Theoretically to improve resolution the width of a pulse can be decreased as far as the system bandwidth will allow (bandwidth ~ 1/pulsewidth). If, however, the system has sufficient bandwidth, a signal with a pulse width small enough to take advantage of the system bandwidth is likely to have a problem with available energy. The signal level could be raised to compensate for lack of signal extent, but that would raise problems of overdriving system components, i.e., large peak power. Pulse compression wave forms allow the use of large bandwidths without having to shorten the pulsewidth. These large time-bandwidth signals provide responses at the processor comparable to that of simple square pulses of much shorter length, hence the name pulse compression (see Fig. 14).

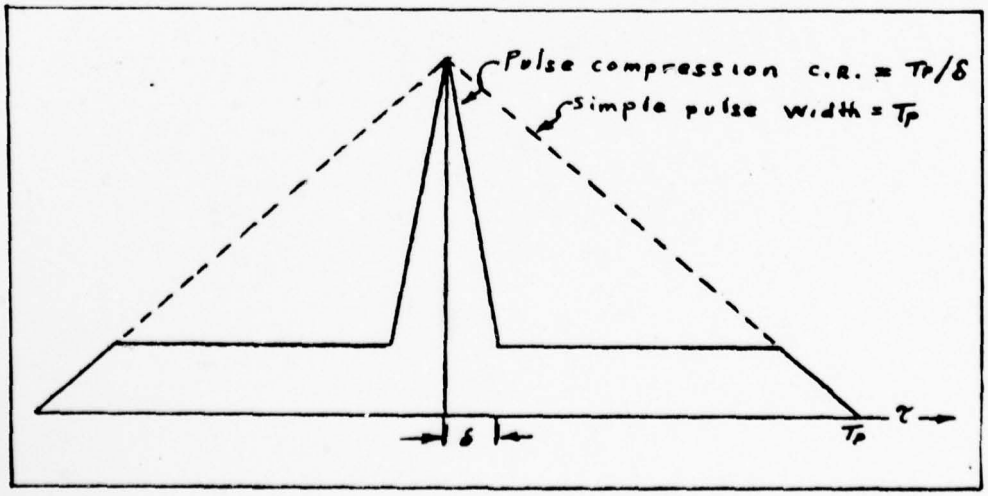

Figure 14. Simple Pulse Vs. Pulse Compression

With pulse compression waveforms the bandwidth (and hence the resolution) can be treated independently of the signal extent. The linear FM waveform is a pulse compression waveform with some interesting and useful characteristics. It is a frequency modulated signal with a linear increase in frequency with time over the length of a pulse, T_p (see Fig. 15).

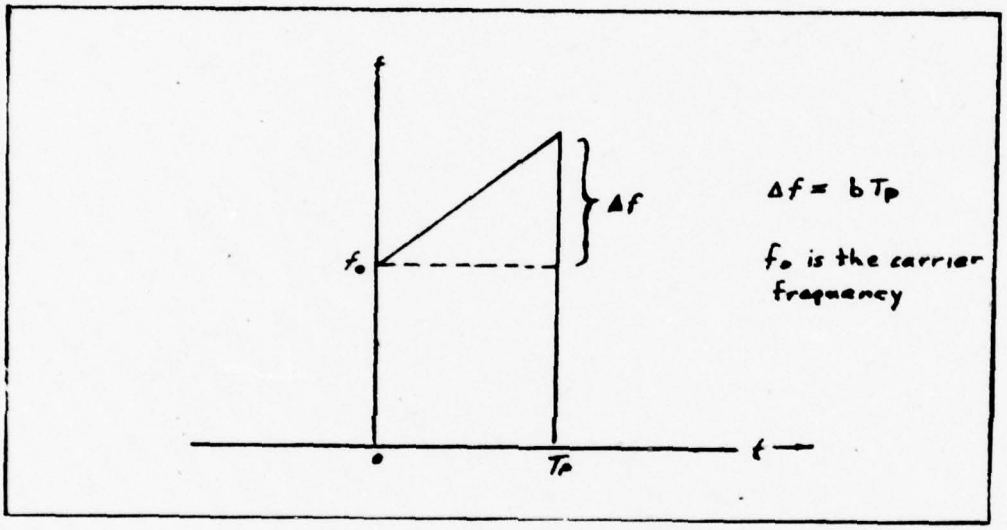

Figure 15. Frequency Sweep in Linear FM

It can be described as having time dependent quadratic phase variation. The received signal, prior to processing or matched filtering is

$$s(t) = \sqrt{E_r}\, u_n(t) = \sqrt{E_r}\, \frac{1}{\sqrt{T_p}}\, rect\left(\frac{t}{T_p}\right) \exp\left[j\pi b t^2\right] \qquad (77)$$

where

E_r is the energy of the received signal and

T_p is the signal duration.

The function $rect\left(\frac{t}{T_p}\right)$ can be written as

$$rect\left(\frac{t}{T_p}\right) = U(t + T_p/2) - U(t - T_p/2) \qquad (78)$$

where $U(t)$ is the unit step function.

The approximation for the frequency spectrum of the linear FM signal at baseband is

$$S(f) \cong \sqrt{E_c}\left[\frac{1}{\sqrt{bT_p}}\ \mathrm{rect}\left(\frac{f}{bT_p}\right)\right] \exp j\left[-\pi f^2/b - \mathrm{sgn}\, b\,\pi/4\right] \qquad (79)$$

This approximation is valid for sufficiently large time bandwidth products ($TB = bT_p^2$). For our purposes a TB of 10 or more is sufficient.

It is apparent that for large TB products the frequency spectrum is almost rectangular in shape. Certainly the shape is never rectangular but approximates the rectangular shape for extremely large time bandwidth products. The trend for frequency spectrums for signals with TB products of 10, 100, and 1000 are depicted in Fig. 16 (Ref. 5:232).

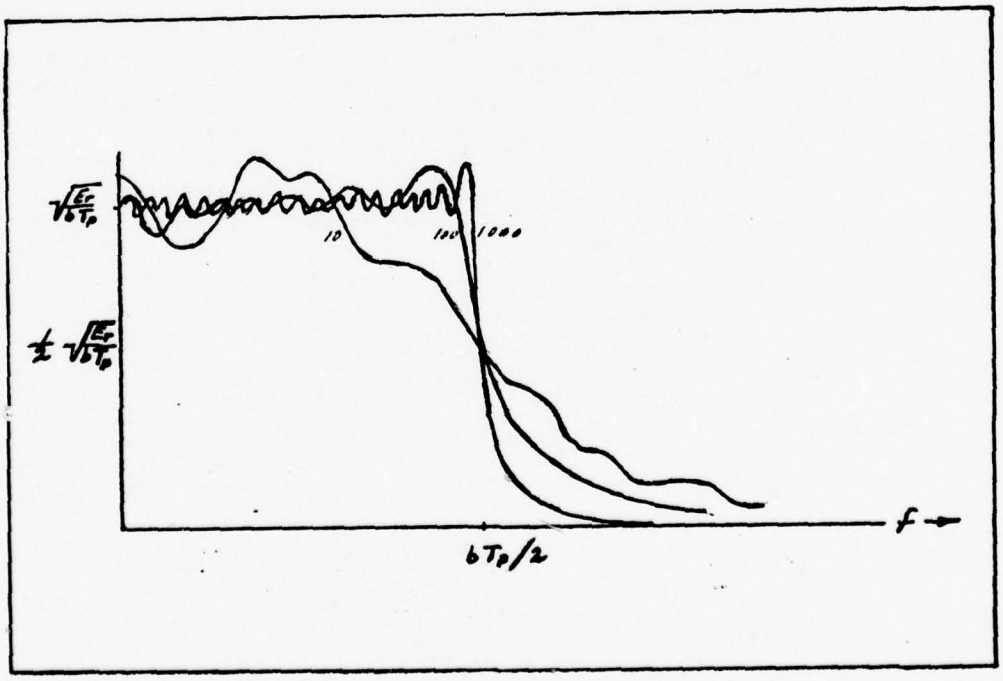

Figure 16. Linear FM Spectrum (TB = 10, 100, 1000)

Bandwidth for the signal previously defined can be taken as bT_p which is the Δf previously described. The mean square bandwidth for linear FM is

$$\beta^2 = \frac{\pi}{3}(bT_p)^2 \tag{80}$$

or

$$\beta^2 = \frac{\pi}{3}(\Delta f)^2 \tag{81}$$

Now that bandwidth and mean square bandwidth have been defined it might be useful to define the pulse compression ratio and relate it to mean square bandwidth. The compression ratio is the ratio of the signal pulsewidth to the effective pulsewidth as seen by the matched filter processor. It is one measure of the resolution (time delay) capabilities of the system and is approximately equal to the time bandwidth product, for L-FM it is

$$(CR) = T_p \Delta f \tag{82}$$

or

$$(CR) = bT_p^2 \tag{83}$$

The ambiguity function, as was mentioned earlier, is very useful in determining the suitability of various waveforms for particular ranging applications. Such issues as target resolution, troublesome sidelobes, doppler sensitivity, potential for masking weak targets with extended ambiguity pedestals can be addressed graphically. The ambiguity function for linear FM (Ref. 5:170) is

$$|\chi(\tau, f_d)| = (1 - |\tau|/T_p)\sin\{[\pi b\tau - \pi f_d][T_p - |\tau|]\}/\{[\pi b\tau - \pi f_d][T_p - |\tau|]\} \tag{84}$$

$|\chi(\tau, f_d)|$ has a sinx/x form along the τ axis. For any doppler mismatch the form (and consequently the peak of the response) is shifted relative to the τ axis. As a result of this $|\chi(\tau, f_d)|$ has a central ridge in the τ- f_d plane. The central ridge has a triangular envelope with a maximum height at τ and $f_d = 0$ and it lies along the line $\tau = \frac{\pi}{b} f_d$. Figure 17 shows some cuts of the ambiguity function taken parallel to the τ axis for various values of f_d .

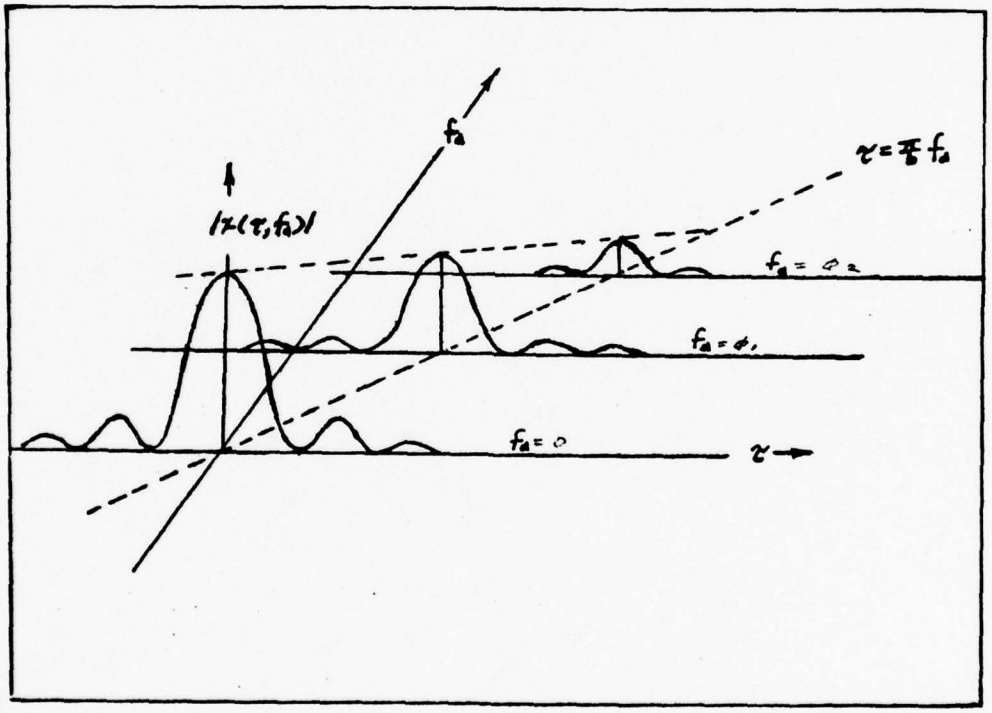

Figure 17. Three Cuts of the Linear FM Response

The delay-doppler coupling shown in Figure 17 is potentially one of the most useful or most troublesome characteristics of the linear FM waveform. For a constant doppler f_d a target at $\tau = 0$ appears to be at $\tau = \frac{\pi}{b} f_d$. Consequently there is a

constant range error or estimate bias. If the doppler frequency is known the range error can be easily compensated for. For the applications considered in this paper the exact range is not as important as an accurate reflection of the relative range from one point (or target) to another. In this case the constant range error is of no great consequence. There may be an added problem of varying doppler but for a scanning system the doppler varies according to a definite scheme. Consequently, compensation for the varying doppler should not be difficult to implement.

Unfortunately a doppler mismatch not only causes a range offset but a decrease in the peak response of the matched filter. The seriousness of a doppler mismatch (or doppler sensitivity) can be determined by finding the value of f_d for which the peak response is 0.707 times the peak response for no doppler shift. This doppler frequency is here designated f_{y_2} and

$$f_{y_2} = b\,\tau_m \tag{85}$$

where τ_m is the position of the peak response relative to the τ axis for a doppler mismatch f_{y_2} . The response at this point is

$$|\chi(\tau_m, f_{y_2})| = \left|1 - \frac{\tau_m}{T_p}\right| = 0.707 \tag{86}$$

and

$$\tau_m = T_p\, 0.29 \tag{87}$$

If the value for τ_m in terms of f_{y_2} is substituted we have

$$f_{1/2} = 0.29\, b T_p \tag{88}$$

and finally

$$f_{1/2} \cong 0.3\, b T_p = 0.3\, \Delta f \tag{89}$$

It appears that a doppler frequency of nearly a third of the signal bandwidth can be tolerated for sufficiently strong signals. It must be pointed out, however, that the width of the mainlobe will not be as narrow as it would for no doppler frequency.

Some reasonable simplifications at this point will facilitate further study of the behavior of the ambiguity function. One such simplification is neglecting the effect of $1 - |\tau|/T_p$. Since it causes a very slow change in $|\chi(\tau, f_d)|$. Then $|\chi(\tau, f_d)|$ can be written (Ref. 5:171)

$$|\chi(\tau, f_d)| = \left| \frac{\sin[\pi T_p (f_d + b\tau)]}{\pi T_p (f_d + b\tau)} \right| \tag{90}$$

and for no doppler mismatch

$$|\chi(\tau, f_d)| = \left| \frac{\sin[\pi b T_p \tau]}{\pi b T_p \tau} \right| \tag{91}$$

It is apparent from Equation (91) that the main lobe has a width, from null to null of

$$\Delta\tau = \frac{1}{b T_p} = \frac{1}{\Delta f} \tag{92}$$

and the resolution in time delay is

$$\tau_r = \frac{1}{\Delta f} \tag{93}$$

Resolution is here defined as width of the mainlobe at half the maximum height.

The final important aspect of $|\chi(\tau, f_d)|$ to be discussed here is the level of the sidelobes. The detrimental impact of sidelobe too high cannot be overstated. With the presence of significant noise the sidelobes could be raised as high or higher than the main lobe and if that were the case the sidelobes would be indistinguishable from the main lobe. The result is considerable uncertainty in determining the position of the target. The primary sidelobe occurs at

$$\tau = \frac{3}{2b} T_p \tag{95}$$

The value of the ambiguity function at this point is

$$|\chi_s| = \left(1 - \frac{\tau_s}{T_p}\right) \frac{2}{3\pi} \tag{96}$$

and with substitution of Equation (95)

$$|\chi_s| = \left(1 - \frac{3}{2bT_p^2}\right) \frac{2}{3\pi} \tag{97}$$

Since $3/2bT_p^2$ is generally quite small (especially for large TB signals)

$$|\chi_s| \cong \frac{2}{3\pi} = 0.21 \tag{98}$$

It appears then that the primary sidelobes are about one fifth the height of the main lobe. In addition to this the primary lobes are close to the main lobe and subsequent lobes are smaller and taper off rapidly.

The Cramer Rao Bound (or lower limit) for range and reflectance estimation provide a good basis for comparing signal performance in parameter estimation. It also gives an indication of which signal parameters affect performance and how they affect performance. The symbol σ^2 will be used here to represent the Cramer Rao Bound and not the actual estimate error. For time delay estimation

$$\sigma_\tau^2 = \frac{h f_o}{4 \eta E_r \beta^2} \tag{99}$$

and since

$$\beta^2 = \frac{\pi}{3} (\Delta f)^2 = \frac{\pi}{3} (b T_p)^2 \tag{100}$$

$$\sigma_\tau^2 = \frac{3 h f_o}{4 \pi \eta E_r (b T_p)^2} \tag{101}$$

Now range and time delay are related by

$$R = (c/2) \tau \tag{102}$$

Therefore for range estimation

$$\sigma_R^2 = \left(\frac{c}{2}\right) \sigma_\tau^2 \tag{103}$$

and

$$\sigma_R^2 = \left(\frac{c}{2}\right)^2 \frac{3 h f_o}{4 \pi \eta E_r (b T_p)^2} \tag{104}$$

and finally for reflectance estimation (ρ)

$$\sigma_\rho^2 = \frac{h f_o}{4 \eta E_r} \tag{105}$$

In the previous sequence of equations the one factor that is unique to linear FM is the mean square bandwidth. Because of this, the signal parameters upon which the mean square bandwidth

depends are of particular importance. For linear FM Δf is the important parameter and an assessment of the system performance required to provide this Δf provides one means of comparing linear FM to other signals.

In the following section binary phase code is discussed and the conclusions for estimation performance are very similar to those for linear FM.

Binary Phase Code. A binary phase coded (or phase reversal coded) signal consists of separate major pulses or code sequences of length T_p . These sequences are made up of subpulses of length δ . Each of the subpulses in a sequence have a phase of zero or π with respect to some constant reference for the sequence. The subpulses are contiguous making the sequence a continuous, constant amplitude signal of binary information. For a sequence with a carrier frequency the subpulses can be considered as constant amplitude pulses multiplied by a plus or minus one. Two such sequences of particular interest are the maximum length (or M) sequence and Barker Codes.

The maximum length sequence is an example of a shift register sequence because it can be generated by a shift register as shown in Figure 18.

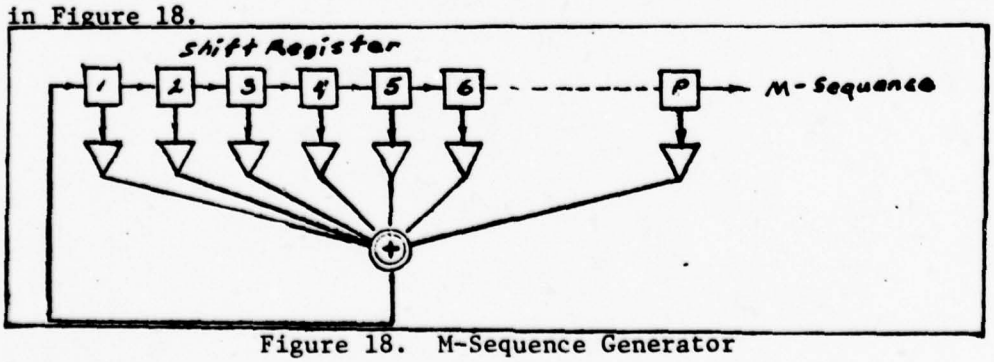

Figure 18. M-Sequence Generator

For P register positions the maximum number of binary combinations possible (before a series of combinations repeats itself) is $2^P - 1$. The combination consisting of all zeros is not allowed because it would continue to repeat itself once its in the register. The feedback arrangement can be chosen to generate a full range of binary combinations (the system output for this would be the M or maximum length sequence) or a partial range of combinations (i.e., less than $2^P - 1$). The M-sequence is generated in this manner because this single closed system can produce a repeatable deterministic sequence of one's and zero's which has all the characteristics of a random sequence of one's and zero's. For this reason the maximum length sequence is also called a pseudonoise code and characterized as being pseudorandom (Ref. 7:7-12). The received signal is

$$\sqrt{E_r}\,\frac{1}{\sqrt{T_p}}\sum_{k=0}^{N-1} a_k \operatorname{rect}\left(\frac{t-k\delta}{\delta}\right), \quad a_k = \pm 1 \tag{106}$$

Here N is the number of subpulses of length δ and

$$N = 2^P - 1 \tag{107}$$

also

$$T_p = N\delta \tag{108}$$

The bandwidth of the signal is on the order of $1/\delta$ and as might be expected the signal will provide the type of resolution in time that would be expected of a single pulse of width δ. This is evident in the ambiguity function (Ref. 6:251).

$$|\chi(k,0)| = \begin{cases} 2^n - 1 & k = 0 \\ 1 & k \neq 0 \end{cases} \qquad (109)$$

Here k represents multiples of δ (i.e., $\tau = k\delta$) along the axis (Fig. 19).

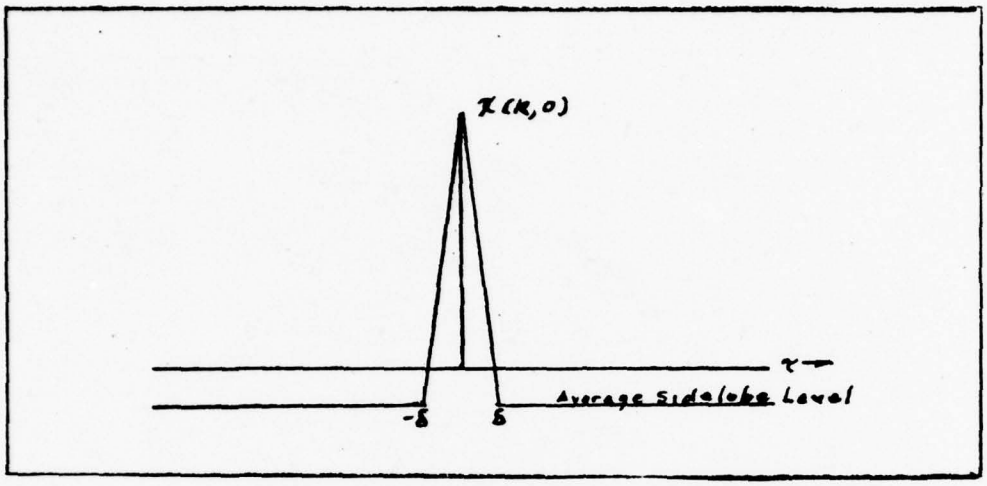

Figure 19. PN Code Ambiguity Function

The average sidelobe level of 1 is possible only if the sequence is cyclic, that is the signal sequence must be continuously repeated to maintain the sidelobe level. If the cycle is truncated (only one sequence) the matched filter response will have a number of sidelobes higher than the average level and some very much higher. A careful selection of the coded sequence can allow selective positioning of the troublesome sidelobes. As a final note on sidelobes the average level is 1/N times the height of the mainlobe.

M-sequences are particularly sensitive to doppler mismatches. The width of the mainlobe of the ambiguity response in doppler is dependent on sequence length and not the subpulse width. It has a width at half maximum of approximately $1/N\delta$ or $1/\tau_p$, and a width from null to null of $2/\tau_p$ (Ref. 5:215). The doppler frequency f_{y_2} can be approximated

$$f_{1/2} = 0.6\left(\frac{1}{T_p}\right) \tag{110}$$

And in terms of bandwidth (BW)

$$f_{1/2} = \frac{0.6}{N}\left(\frac{1}{\delta}\right) \cong \frac{0.6}{N}(BW) \tag{111}$$

Perhaps more important is the fact that the response drops off extremely fast for frequencies past $f_{1/2}$.

Binary phase coded sequences employing Barker codes have uniformly low sidelobes. For a sequence of N elements the sidelobes are less than or equal to 1/N times the height of the mainlobe. Because of the uniform sidelobes Barker Codes are classified as optimum. There are seven known Barker codes, including Barker codes with lengths of 2, 3, 4, 5, 7, 11, or 13 elements. For Barker codes $|\chi(\tau, 0)|$ may be written (see Fig. 20) (Ref. 6:245)

$$|\chi(k,0)| = \begin{cases} N, & k=0 \\ 1 \text{ or } 0, & k \neq 0 \end{cases} \tag{112}$$

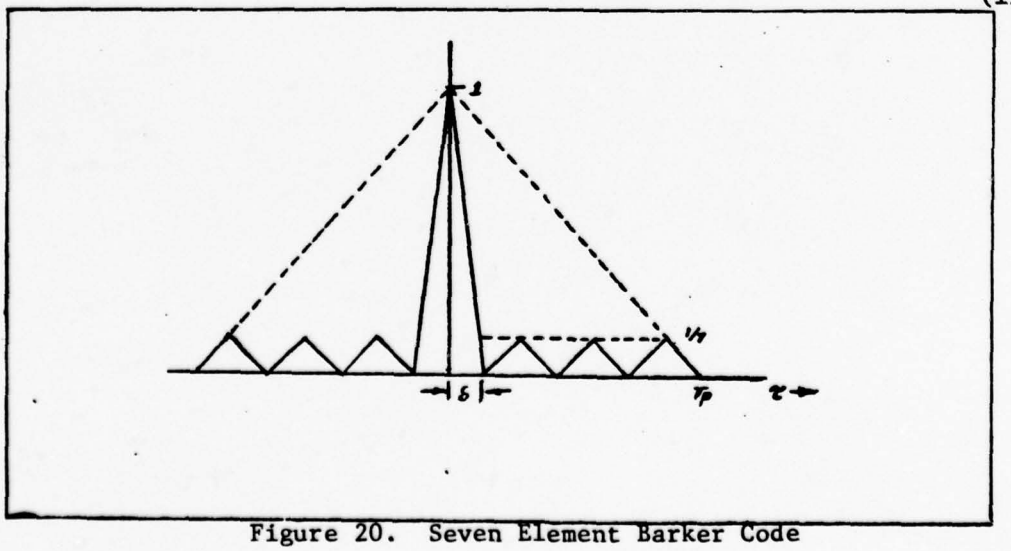

Figure 20. Seven Element Barker Code

Time resolution and doppler sensitivity characteristics of the Barker coded sequence are the same as for the M-sequences. They have the same dependence on sequence length and subpulse width. They also have the same parameter estimation performance. The mean square bandwidth is dependent on the subpulse width. It is calculated by approximating the square pulse with a gaussian pulse.

$$U_p = e^{-t^2/2\delta^2} \tag{113}$$

This yields

$$\beta^2 = \frac{1}{\sqrt{8}\,\delta^2} \tag{114}$$

For both Barker coded sequence and M-sequences the Cramer Rao Bound for time delay estimates is

$$\sigma_\tau^2 = \frac{hf_o}{4\eta E_r \beta^2} = \frac{hf_o \sqrt{8}\,\delta^2}{4\eta E_r} \tag{115}$$

and for range

$$\sigma_R^2 = \left(\frac{c}{2}\right)^2 \frac{hf_o \sqrt{8}\,\delta^2}{4\eta E_r} \tag{116}$$

and the Cramer Rao Bound for reflectance is

$$\sigma_\rho^2 = \frac{hf_o}{4\eta E_r} \tag{117}$$

Here once again we see that mean square bandwidth is the significant variable parameter. It is the one parameter uniquely related to a signal type. The mean square bandwidth for this case is determined by subpulse width. The importance of signal bandwidth cannot be overstated. It is apparent not only in the pulse

compression waveforms but also in the sinusoidal AM signal discussed in the next section.

Sinusoidal Amplitude Modulation. A continuous signal with sinusoidal amplitude modulation can be used to obtain very accurate range estimation. Range estimation is achieved by estimating the phase of the return signal or rather the phase change the amplitude of the transmitted signal undergoes in the time it takes for the signal to travel to the target and back. For a signal of frequency f_m (i.e., modulation frequency) the round trip target to transmitted distance $2R$ can be related to the phase change ϕ by the equation

$$2R = \frac{\phi c}{2\pi f_m} \tag{118}$$

Therefore

$$R = \frac{\phi c}{4\pi f_m} \tag{119}$$

Analysis of optimum processing for phase estimation will show that the maximum likelihood estimator is the phase lock loop (Ref. 8:408). A phase lock loop and an envelope detector can be used to determine the phase or phase variation of the sinusoidal AM signal at the receiver IF frequency (or the output of the receiver IF filter). Figure 21 shows a schematic of the envelope detector and the phase-lock-loop.

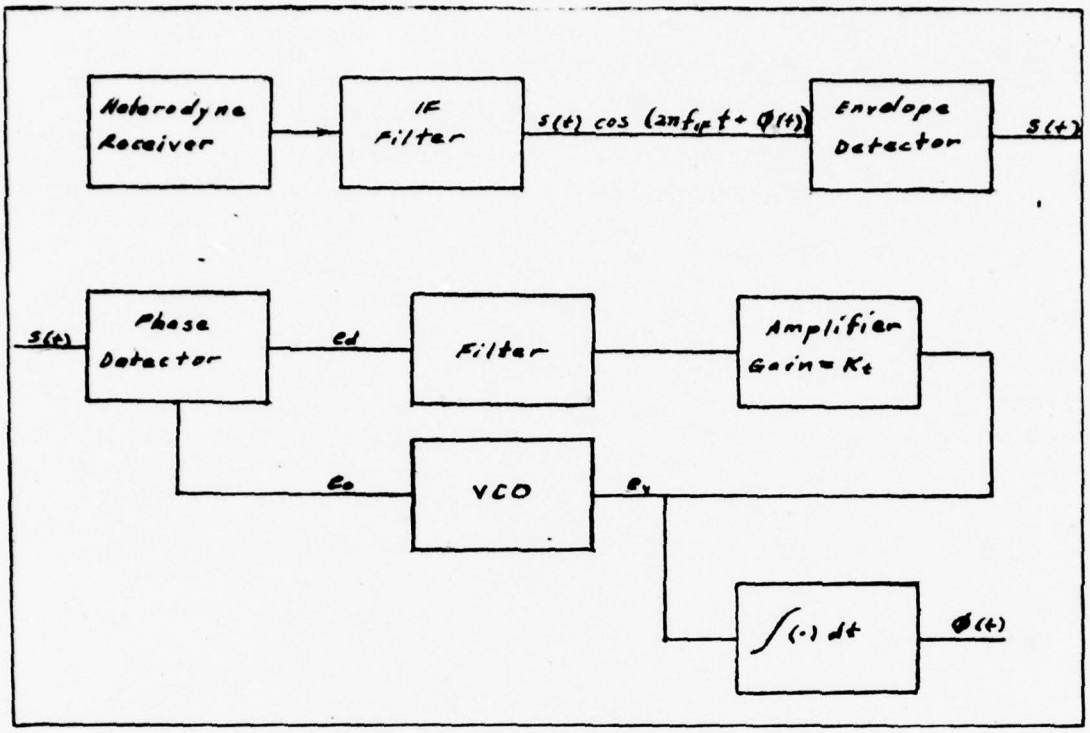

Figure 21. Detector and Phase Estimator

The envelope detector is used to remove the IF carrier from the signal. The signal from the envelope detector with noise may be characterized by

$$r(t) = \sqrt{[s(t) + n_c(t)]^2 + n_s^2(t)} \tag{120}$$

Here $n_c(t)$ and $n_s(t)$ are the quadrature components of noise from the heterodyne receiver and IF filter. For sufficiently large signal-to-noise ratio

$$|s(t) + n_c(t)| >> |n_s(t)| \tag{121}$$

and

$$r(t) \cong s(t) + n_c(t) \tag{122}$$

Therefore the output of the envelope detector is the signal with additive noise $n_c(t)$. This noise has twice the spectral height, but one half the bandwidth of the input noise. Consequently the total noise power is unchanged (Ref. 8:268).

The signal into the phase lock loop (Fig. 21) has the form

$$S(t) = \sqrt{2}\sqrt{P_r}\cos[2\pi f_m t + 2\pi f_d t + \phi(t)] \tag{123}$$

Here f_d is the frequency change due to the doppler effect. The doppler effect simply causes a steady-state phase error. For a system employed to establish a point to point range deviation for an extended target, a steady-state error is not a critical factor. The mean square phase error is the important performance measure. This is

$$\sigma_\phi^2 = \frac{N_0}{2P_r} W_L \tag{124}$$

or

$$\sigma_\phi^2 = \frac{hf_0}{4\eta P_r} W_L \tag{125}$$

W_L is the loop bandwidth and is approximately equal to $1/T_p$ Here T_p is the dwell time. The mean square phase error can now be expressed as

$$\sigma_\phi^2 = \frac{hf_0}{4\eta P_r T_p} \tag{126}$$

and since

$$R = \frac{\phi c}{2\pi f_m} \tag{127}$$

the mean square error for range is

$$\sigma_R^2 = \left(\frac{c}{2\pi f_m}\right)^2 \frac{h f_o}{4\eta P_r T_p} \tag{128}$$

since

$$E_r = P_r T_p \tag{129}$$

The mean square error for range is

$$\sigma_R^2 = \left(\frac{c}{2}\right)^2 \frac{h f_o}{4\eta E_r (2\pi f_m)^2} \tag{130}$$

The sinusoidal AM signal appears also to have an estimation accuracy which depends on a quantity which can be described as mean square bandwidth.

Coherent Pulse Trains. A simple means of extending the duration of a signal without sacrificing bandwidth is repetition of the signal at regularly or irregularly spaced intervals. In this case the signal is a very narrow pulse. With a few exceptions, which will be pointed out, the coherent pulse train provides the same performance as the binary phase coded signals.

The difference in the matched filter response for the binary phase coded signals and the coherent pulse train signals are primarily in the sidelobe characteristics. The uniformly spaced pulse train has a set of high sidelobes. These sidelobes can in fact be considered ambiguities. That is they are so high that with noise added they can be easily mistaken for the mainlobe. If the pulse train has a length of T_p and subpulse width of the ambiguity function would be similar to that shown in Fig. 22.

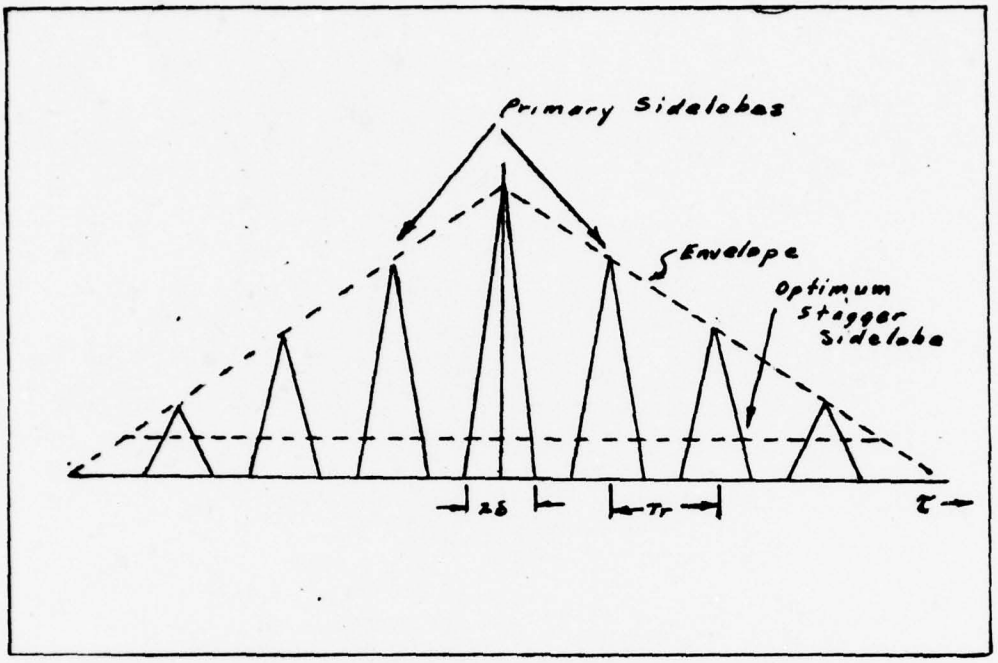

Figure 22. Coherent Pulse Train Ambiguity Function

In Fig. 22 T_r is the repetition interval for the subpulses and the envelope of the pulses is the shape of the ambiguity function for a single continuous pulse of length T_p.

The ambiguities can be removed by staggering the interval T_r. There are two types of staggered pulse trains that may be employed. They are optimum and suboptimum. The difference is that the optimum staggered pulse train produces a uniformly low sidelobe level the height of which depends on the number of pulses in the train and there are a limited number of them. Sidelobes of the suboptimum staggered pulse train are not uniform and may in fact be very high at some points in the $\tau - f_d$ plane for some staggered pulse arrangements. Regardless of whether suboptimum

or optimum stagger is used, there will be a greater amount of time during which no signal is transmitted than there would be for uniformly spaced pulse trains, and even for the uniform pulse trains in most cases the transmission intervals are smaller than the nontransmission intervals. This translates into loss of available power for transmission and a requirement to absorb or deflect a considerable amount of energy.

Because of its simplicity and its smaller cost in loss of available power compared to optimum staggered pulse, the uniform pulse train is given further consideration here. As pointed out previously, a major problem with uniform pulse trains is the closeness of the ambiguities or sidelobes. Consider, for example, a pulse train with a subpulse repetition rate interval (T_r), equal to twice the subpulse width (δ) as shown in Fig. 23.

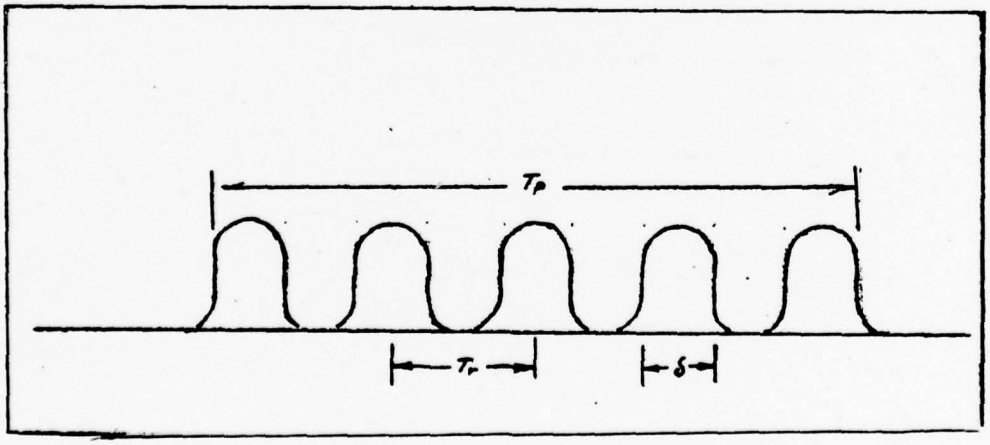

Figure 23. Uniform Pulse Train

This particular arrangement was chosen for discussion because it provides the same power as a sinusoidal signal of comparable height. For this arrangement the ambiguities are spaced 2δ apart. In terms of round trip distance ΔR

$$2\Delta R = 2\delta C \tag{131}$$

and

$$\Delta R = \delta C \tag{132}$$

The pulses as shown in Fig. 23 and as can be expected in practical situations are not quite rectangular and since it also simplifies the problem of determining bandwidth the pulses will be considered approximately gaussian. Certainly the pulses generated by any practical systems will approximate a gaussian form a lot closer than a rectangular form. For pulsewidth δ the bandwidth is approximately π/δ and the total distance between ambiguities in terms of bandwidth is

$$\Delta R = \frac{C\pi}{W_o} \tag{133}$$

Here W_o is the bandwidth of the individual subpulse. In general if

$$T_r = N\delta \tag{134}$$

then

$$\Delta R = \frac{N}{2}\frac{C\pi}{W_o} \tag{135}$$

If the target space for a particular ranging application does fall within the primary sidelobes, the uniform pulse train can be a viable modulation alternative. It allows the added flexibility of trade-offs which don't affect pulsewidth (resolution or bandwidth). Consider for example a ranging application for which a fixed sequence time and a fixed subpulse width is desired. If the target space allows the subpulse repetition interval can be

decreased to a value less than twice the subpulse width which will provide more energy to the receiver for each sequence. If on the other hand the target space requires a larger repetition interval and the laser average power level is high enough, the repetition interval can be increased.

The uniform pulse train provides the same resolution as binary phase coded sequences of comparable subpulse width and has the same problem with sensitivity of the matched filter response level to doppler shifts. If instead of synchronous detection, envelope detection is used prior to matched filtering the doppler problem is eliminated. The envelope will remove the IF carrier regardless of its frequency and the pulse train can be matched filtered at baseband. This can be a very important consideration for an airborne transmitter.

The primary problem with using the uniform pulse train is close ambiguity in time delay and with the optimum staggered pulse loss of available energy due to the intervals between subpulses is a problem. A compromise between these two could be very useful. A limited form of pulse stagger may be employed. If the staggering scheme is chosen so that the number of pulses in a sequence is the same as would be used for a uniform pulse train then no energy is sacrificed. The scheme should be carefully chosen to either reduce the primary sidelobes or increase the separation of the mainlobe and primary sidelobes.

Signal Generation and Recovery

Perhaps as important as the signal characteristics are the system requirements for generation and recovery of the modulation waveform. The remainder of this section will address the matter of generation and recovery.

Linear FM. There are two means commonly used to effect frequency change in the laser output. One method is to physically change the separation distance of the end mirrors. This can be done by mounting the 100% reflecting mirror on a piezoelectric crystal. A voltage applied to the crystal causes deformation of the crystal and moves the mirror. The other method is to change the effective optical path in the laser especially by changing the index of refraction of a gas or crystal within the cavity.

A major problem associated with this type of modulation is frequency jumping. Unplanned frequency shifts on the order of 1 MHz can be expected. For small bandwidth signals this can represent a serious alteration of the modulation scheme. At the receiver the effects would be increased sidelobes in the matched filter response, a decrease in the height of the response and spreading of the mainlobe. If the bandwidth of the signal is 10 MHz or more the mismatch at the filter should be tolerable. This conclusion is based on the fact that the Linear FM filter can accept a mismatch of nearly one-third the signal bandwidth before the peak response is reduced to one-half. Besides the frequency jumping there is the problem of insuring that the induced frequency change Δf follows the desired range of frequencies

from pulse to pulse. Problems such as these place the added demands of sampling and feedback control on the systems.

Regardless of the type of modulation used the maximum frequency range possible is the frequency difference between two axial modes in the laser (Ref. 10:114). This frequency difference is

$$\Delta f = \frac{c}{2\ell c} \tag{136}$$

If the laser cavity is one meter long the maximum frequency change possible (Δf) is 150 MHz. The Δf available with practical modulators (either intracavity or extracavity) is much less than 150 MHz. Values of less than 10 MHz to a few tens of MHzs are common (Ref. 10:144). (A requirement of Δf approaching 100 MHz would be a very stringent demand on the system.)

The heterodyne receiver should handle the largest Δf produced by the FM transmitter. Bandwidths in excess of 1 GHz for HgCdTe detectors at 10.6 μ have been measured (Ref. 10:114) and responses out to 3 GHz are predicted. For good detectors frequency responses of 300 MHz to 500 MHz are reasonable values. For electro-optic modulators the modulation rates available (not to be confused with the Δf of the FM signal) are of the same order of magnitude as the responses available with IR detectors. A modulation bandwidth in excess of 1 GHz has been measured and even higher values predicted (Ref. 11:227).

At the receiver the FM signal must either be recovered before matched filtering or matched filtered at the intermediate frequency. In either case the uncertain phase of the receiver

field is an extremely troublesome complicating factor for the receiver. The amplitude of the signal recovered from the synchronous detector varies as the cosine of the phase difference between the IF signal and the detector reference. The result is a recovered signal with unwanted amplitude modulation which can reduce the signal to extremely low levels. Regardless of this the simple variation of the signal level is enough of a problem. The solution to this problem would involve feedback circuitry to sample the frequency and phase of the detected signal and modify the local source to match the signal.

Phase Modulation. Phase modulation of a laser beam can be accomplished with an extracavity electro-optic modulator consisting of an electro-optic crystal and a polarizer.

The signal applied to the electro-optical crystal is binary. It consists of a chain of contiguous pulses each of which is at one of two possible voltage levels. The voltage levels are of course chosen to produce the desired phase changes. A particularly important consideration for this type of modulation is that, for the ranging application being considered and the codes being considered, a high switching rate is required. For example, if a bandwidth of 500 MHz is to be used then a subpulse rate of 5×10^8 per second is required. This is a fairly high switching rate for electro-optic crystals. At this rate light propagation time through the crystal and power loss in the crystal (which is proportional to the square of the switching rate) adversely affects the modulated field.

Another problem to contend with besides generation of the modulation scheme, is maintenance of the phases of the individual subpulses relative to a constant reference in accord with the desired phase code of the sequence of subpulses. When the sequences are repeated continuously, a phase shift of the laser output (loss of coherence) prior to the modulation prevents the modulator from producing the desired code. In other words the phase shift if it occurs during a sequence alters the coce of the sequence. In addition to this atmospheric effects and reflection at the target work to alter the nature of the coded sequences. The end result is a mismatch at the matched filter.

Just as with the L-FM signal the phase coded signal could be recovered through synchronous detection prior to matched filtering. The detector must then be designed to handle the phase matching problem and it must do so without altering the nature of the code of the sequence.

Sinusoidal Amplitude Modulation. Amplitude modulation is the simplest form of modulation considered here and it provides the fewest complications. The modulation of the field is not altered by phase changes due to reflectance and atmosphere effects and since envelope detection is used to recover the modulation signal, phase of the received field is not important. One problem for amplitude modulated signals is fluctuation of the field power due to atmospheric turbulence. However, the fluctuations, if they exist, would be very slow compared to the

modulating signal and consequently would not seriously distort the modulation. A limiter in front of the envelope detector can remove the effects of the field fluctuations.

V. CONCLUSION

Performance analysis of the various signal types indicates that there are two signal/system characteristics which impact the accuracy of range estimation. These are signal bandwidth and the ratio of noise spectral density to signal energy (Snf/Er). For the signal types considered here these are determined or limited by the particular ranging application and the system hardware. Specifically transmitter power will limit Er, modulator and detector will limit available bandwidth for the signal, and detector characteristics will determine noise spectral density. If advantage is taken of the available transmitter power and system bandwidth then signal bandwidth and Snf/Er will be of the same order of magnitude for each signal type and consequently the ranging accuracies will be the same with the exception of the amplitude modulated signals.

The amplitude modulated signals have less energy than that provided by the laser and if 100 percent modulation is used the available power is decreased by 50%. Despite this the sinusoidal amplitude modulation is predicted to have an estimation error ~ 2 times that of the pulse compression waveforms.

The various signal types discussed here can be compared in a number of ways and each of the comparisons have the potential of providing data useful to the systems planner, for signal selection. One comparison involves estimation accuracy. Given that parameters such as signal energy, signal bandwidth and

temporal extent are constant for the signals a comparison can be made based on the manner in which the previously mentioned affect the signal accuracy. Accuracy is an important criterion but it cannot be considered alone particularly when the predicted accuracies of various signals are of the same order of magnitude. A more useful selection process would include comparisons of problems associated with the signals, such as sidelobes and ambiguities; limitations of the signals, such as maximum achievable bandwidth and systems complications such as those involving signal detection. The comparison begins here with estimation accuracy.

For pulse compression waveforms the estimation accuracy can be expressed in terms of three quantities. These are noise spectral density (Sn(f)), the energy (Er) of the received signal and the mean square bandwidth (β^2) of the signal and they are related by the equation $\sigma_R^2 \geq \frac{Sn(f)}{E_r \beta^2} \left(\frac{c}{2}\right)^2$. These three parameters are determined by system limitation. Signal energy (Er) is determined by transmitter limitations and Sn(f) is determined by detector characteristics.

Similarly for sinusoidal AM, $\sigma_R^2 \geq \left(\frac{c}{2}\right)^2 \frac{Sn(f)}{E_r (2\pi f_m)^2}$. The quantity $(2\pi f_m)^2$ is the mean square bandwidth for sinusoidal AM. What the error estimates show is that the accuracy of each of the signals have the same dependence on the same three system parameters.

The value of the FM signal is in its ability to provide resolution associated with large bandwidth without troublesome time delay ambiguities. In addition it can tolerate large doppler shifts unlike the binary phase codes. However, lasers will allow only a small bandwidth via frequency modulation (i.e., compared to the total modulation bandwidth available through electro-optic modulators). Because of the limitations on frequency modulation in lasers linear FM can be restricted to consideration for signal bandwidths less than 50 MHz.

The major advantage that linear FM offers over the AM signal, uniform pulse train and sinusoidal AM, is its lack of troublesome ambiguities. For bandwidths less than 50 MHz, to which LFM is limited, the ambiguities associated with the AM signals no longer present an intractable problem. In fact the ambiguities will be sufficiently separated to suit most of the target distributions of interest. Thus for this range of bandwidths linear FM loses its major advantage.

The AM signals on the other hand do retain some important advantages over linear FM. The signals are simpler to generate and the system used to recover and process the signals is simpler. Besides this the AM signals suffer less from transmission effects. Specifically since the signals can be recovered by envelope detection, the phase of the optical carrier and doppler effects on the optical carrier are of no consequence. A linear FM or binary phase code system would have to be designed to compensate for doppler shifts, uncertain phase or phase mismatch.

Either of the two AM signals (uniform pulse and sinusoidal) would satisfy the requirement of this ranging application and the choice should be made between the two. There are a number of considerations to be made in making a choice. First, for any bandwidth limit sinusoidal AM is more accurate. The uniform pulse train on the other hand has more widely separated ambiguities and there is the added flexibility of being able to employ some form of staggering to modify the nature of the sidelobes. The principal goal of course would be to increase separation of the main lobe and the first sidelobes. In fact, if there is sufficient power to allow wide separation of pulse, a carefully selected staggered pulse train could produce sufficient ambiguity separation even for bandwidths greater than 50 MHz.

Sinusoidal AM appears most promising for near-term system implementation. This is mainly because of the simplicity of the system requirements and the fact that the systems difficulties that may be encountered are predictable and surmountable (not like the phase problems with linear FM).

Bibliography

1. Skolnik, Merrill II, et al. Radar Handbook. New York: McGraw-Hill Book Co., 1970.

2. Berger, F. B. "The Nature of Doppler Velocity Measurement." IRE Transactions on Aeronautical and Navigational Electronics, 103-112 (September 1957).

3. Van Trees, Harry L. Detection, Estimation, and Modulation Theory Part I. New York: John Wiley and Sons, Inc., 1968.

4. Van Trees, Harry L. Detection, Estimation, and Modulation Theory, Part III. New York: John Wiley and Sons., Inc., 1971.

5. Rihaczek, August W. Principles of High Resolution Signals. New York: McGraw-Hill Book Co., 1969.

6. Cook, Charles E. and Marvin Bernfeld. Radar Signals. New York: Academic Press, 1967.

7. Golomb, Solomon W., et al. Digital Communications. New Jersey: Prentice-Hall, Inc., 1964.

8. Ziemer, R.E. and W. H. Tranter. Systems, Modulation, and Noise. Boston: Houghton Mifflin Co., 1976.

9. Duley, W. W. CO_2 Lasers Effects and Applications. New York: Academic Press, 1976.

10. Verie, Christian and Michel Sirieux. "Gigahertz Cutoff Frequency Capabilities of Cd Hg Te Photovoltaic Detectors at 10.6 Microns." IEEE Journal of Quantum Electronics QE-8, No. 2: 255-244 (February 1976).

11. Kiefer, James E., et al. "Intracavity Cd Te Modulators for CO_2 Lasers." IEEE Journal of Quantum Electronics, QE-8, No. 225-244 (February 1976).

12. McElroy, John H., et al. "CO_2 Laser Communications Systems for Near-Earth Space Applications." Proceedings of the IEEE Vol. 65, No. 2:221-250 (February 1977).

VITA

Willie B. Townsend was born on 22 August 1949 in Osceola, Arkansas. He graduated from high school in Memphis, Tennessee and attended Memphis State University from which a degree of Bachelor of Science in Electrical Engineering was received on 6 May 1972. Upon graduation, he received a commission in the USAF through the ROTC program. He has served as a project engineer for various sytems acquisition programs for the USAF until entering the School of Engineering, Air Force Institute of Technology, in June 1976.

UNCLASSIFIED

(14) AFIT/GEO/EE/77-7

SECURITY CLASSIFICATION OF THIS PAGE (When Data Entered)

REPORT DOCUMENTATION PAGE

READ INSTRUCTIONS BEFORE COMPLETING FORM

1. REPORT NUMBER: GEO/EE/77-7

2. GOVT ACCESSION NO.: (9) Master's

3. RECIPIENT'S CATALOG NUMBER: thesis

4. (6) TITLE (and Subtitle): ANALYSIS AND COMPARISON OF MODULATION SCHEMES FOR A LASER LINE SCAN SYSTEM AT 10.6 MICRONS.

5. TYPE OF REPORT & PERIOD COVERED: MS Thesis

6. PERFORMING ORG. REPORT NUMBER

7. (20) AUTHOR(s): Willie B. Townsend, Captain, USAF

8. CONTRACT OR GRANT NUMBER(s)

9. PERFORMING ORGANIZATION NAME AND ADDRESS: Air Force Institute of Technology(AFIT-EN) Wright-Patterson AFB, Ohio 45433

10. PROGRAM ELEMENT, PROJECT, TASK AREA & WORK UNIT NUMBERS: (12) 75p.

11. CONTROLLING OFFICE NAME AND ADDRESS: (11)

12. REPORT DATE: Dece[illegible]977

13. NUMBER OF PAGES: 73

14. MONITORING AGENCY NAME & ADDRESS(if different from Controlling Office): Air Force Avionics Laboratory(AFAL-RNI) Air Force Systems Command Wright-Patterson AFB, Ohio 45433

15. SECURITY CLASS. (of this report): Unclassified

15a. DECLASSIFICATION/DOWNGRADING SCHEDULE

16. DISTRIBUTION STATEMENT (of this Report)

Approved for public release; distribution unlimited

17. DISTRIBUTION STATEMENT (of the abstract entered in Block 20, if different from Report)

18. SUPPLEMENTARY NOTES

Approved for public release; IAW AFR 190-17

JERRAL F. GUESS, Captain, USAF
Director of Information

19. KEY WORDS (Continue on reverse side if necessary and identify by block number)

Line Scanning
Ranging
Laser Radar

20. ABSTRACT (Continue on reverse side if necessary and identify by block number)

Modulation schemes for a laser line scanning system were analyzed and compared. The comparison involved signal performance in both range and reflectance estimation, limitations associated with particular signal types, and complexity of systems required to generate and process the various signal types. the analysis showed that estimation accuracy depends on signal parameters that are, for the most part, determined by system limitations. The accuracy analysis provided instead an indication of

DD FORM 1 JAN 73 1473 EDITION OF 1 NOV 65 IS OBSOLETE

UNCLASSIFIED

SECURITY CLASSIFICATION OF THIS PAGE (When Data Entered)

012 225

(block 20) which signal parameters are important and the mean square bandwidth proved to be the most important variable signal parameter. Selection of a particular modulation scheme was then based on the demands that a particular signal type at a given bandwidth puts on the generating and processing systems and miscellaneous problems and advantages associated with the signal.